Peripheral opioid receptor antagonism alleviates fentanyl-induced cardiorespiratory depression and is devoid of aversive behavior

[1,2,3]Brian C. Ruyle, [1,2,3]Sarah Masud, [1,2,3]Rohith Kesaraju, [1,2,3]Mubariz Tahirkheli, [1,2,3]Juhi Modh, [1,2,3]Caroline G. Roth, [1,2,3]Sofia Angulo-Lopera, [1,2,3]Tania Lintz, [1,2,3]Jessica A. Higginbotham, [1,2,3]Nicolas Massaly, [1,2,3,4,5]Jose A. Moron*

Affiliations:

[1]Department of Anesthesiology, Washington University in St Louis; St. Louis, MO, USA

[2]Pain Center, Washington University in St Louis; St. Louis, MO, USA

[3]School of Medicine, Washington University in St. Louis; St. Louis, MO, USA

[4]Department of Neuroscience, Washington University in St. Louis; St. Louis, MO, USA

[5]Department of Psychiatry, Washington University in St. Louis; St. Louis, MO, USA

*corresponding author Email: jmoron-concepcion@wustl.edu

ABSTRACT

Millions of Americans suffering from Opioid Use Disorders (OUD) face a high risk of fatal overdose due to opioid-induced respiratory depression (OIRD). Fentanyl, a powerful synthetic opioid, is a major contributor to the rising rates of overdose deaths. Reversing fentanyl overdoses has proved challenging due to its high potency and the rapid onset of OIRD. We assessed the contributions of central and peripheral mu opioid receptors (MORs) in mediating fentanyl-induced physiological responses. The peripherally restricted MOR antagonist naloxone methiodide (NLXM) both prevented and reversed OIRD to a degree comparable to that of naloxone (NLX), indicating substantial involvement of peripheral MORs to OIRD. Interestingly, NLXM-mediated OIRD reversal did not produce aversive behaviors observed after NLX. We show that neurons in the nucleus of the solitary tract (nTS), the first central synapse of peripheral afferents, exhibit a biphasic activity profile following fentanyl exposure. NLXM pretreatment attenuates this activity, suggesting that these responses are mediated by peripheral MORs. Together, these findings establish a critical role for peripheral MORs, including ascending inputs to the nTS, as sites of dysfunction during OIRD. Furthermore, selective peripheral MOR antagonism could be a promising therapeutic strategy for managing OIRD by sparing CNS-driven acute opioid-associated withdrawal and aversion observed after NLX.

Keywords

Opioids, brainstem, respiratory depression, opioid receptors, fentanyl

Significance Statement:

In this study, we compare the central versus peripheral components underlying fentanyl-induced cardiorespiratory depression to prevent overdose deaths. Our data indicate that these effects are, at least partially, due to the activation of mu opioid receptors present in peripheral sites. These findings provide insight into peripheral contributions to fentanyl-induced overdoses and could potentially lead to the development of treatments selectively targeting the peripheral system, sparing individuals from the CNS-driven acute opioid withdrawal generally observed with the use of naloxone.

INTRODUCTION

Millions of Americans live with Opioid Use Disorders (OUD) and face a high risk of opioid-induced respiratory depression (OIRD), the leading cause of opioid related deaths (*1*). The number of fatalities attributed to OIRD has been exacerbated by the rise of distribution and use of synthetic opioids, such as fentanyl (*2*–*5*). Fentanyl is a highly lipophilic opioid that readily crosses the blood-brain barrier and binds tightly to mu opioid receptors (MORs), which are abundant in the respiratory centers of the brainstem (*1*, *6*, *7*). Compared to other opioids such as heroin and morphine, fentanyl exhibits both a faster onset of OIRD and higher potency for MOR binding (*8*, *9*), minimizing successful prevention of lethal outcomes using naloxone (NLX), a competitive and preferential MOR antagonist (*10*, *11*). Despite its high efficacy in reversing OIRD, NLX also precipitates unpleasant withdrawal symptoms and aversion, as reported in patients and preclinical models (*11*–*14*), making its implementation for managing OUD challenging. Therefore, a better understanding of the pharmacology, specific brain regions and pathways, and physiological responses induced by high doses of fentanyl are necessary to develop effective prevention and intervention strategies, ultimately saving lives of patients suffering from OUD.

Several regions have been implicated as key sites of triggering OIRD, including the Pre-Botzinger Complex in the ventral medulla and the parabrachial nucleus and Kölliker-Fuse nucleus in the pons (*1*, *15*–*20*). Opioids act directly within these networks to alter inspiratory and expiratory phase duration, leading to overall reductions in respiratory rate and apneas (*18*, *20*, *21*). In addition, the nucleus of the solitary tract (nTS), located in the dorsal brainstem, is the first central site that receives sensory afferent information via cranial nerves related to cardiorespiratory, gustatory and gastrointestinal function (*22*). Acute hypoxia robustly activates nTS neurons (*23*, *24*) to initiate appropriate autonomic and cardiorespiratory responses that

66 facilitate a return to homeostatic physiological states. MORs are expressed throughout the
67 entire caudal-rostral extent of the nTS, where they are located postsynaptically on nTS neurons
68 and on vagal afferent fibers that terminate within the nTS(*25*–*27*). Opioids induce both systemic
69 and brain hypoxia (*28*, *29*) and produce an increase in Fos-immunoreactivity in the nTS (*26*,
70 *30*). However, engaging MOR signaling in the nTS impairs hypoxic ventilatory responses (*7*).
71 This suggests that OIRD may result from nTS dysfunction failing to engage appropriate
72 cardiorespiratory responses, thereby leading to prolonged OIRD. However, the specific
73 contributions of nTS MOR, including ascending MOR-expressing inputs from the periphery to
74 this region, in driving aberrant cardiorespiratory depression are still not fully understood.
75 In addition to their high expression throughout brainstem respiratory nuclei, MORs are also
76 expressed in the periphery, including sensory ganglia, lung afferents, cardiac tissue and cranial
77 nerves that terminate within the nTS (*31*, *32*). Naloxone Methiodide (NLXM) is a quaternary
78 derivative of NLX that does not cross the blood brain barrier at low doses, making it a useful tool
79 to assess the peripheral vs central contribution of MORs in opioid-induced physiology and
80 behavior (*10*, *33*). Despite its lower binding affinity for MOR (*10*), NLXM has been shown to
81 reverse opioid-induced hypoventilation and brain hypoxia in rodent models (*12*, *33*, *34*),
82 suggesting that peripheral opioid receptors may play a greater role in OIRD than previously
83 thought. However, no studies to date have provided a comprehensive assessment of opioid-
84 induced cardiorespiratory depression and systemic hypoxia combined with a real-time
85 assessment of MOR-mediated activity of nTS neurons.
86 In the present study, we examined the relative contributions of central and peripheral MORs
87 mediating fentanyl-induced depression of cardiorespiratory parameters and investigated
88 potential mechanisms of opioid-induced dysfunction within the nTS. We report that fentanyl-
89 induced cardiorespiratory depression and prolonged systemic hypoxia can be prevented or
90 reversed by NLXM to a comparable degree as NLX. As compared to NLX, NLXM-mediated
91 reversal of OIRD did not produce aversive-like behaviors. Fentanyl induced robust Fos-IR
92 expression in the nTS in a dose-dependent manner, and this activation can be attributed to a
93 combination of direct effects of opioids acting at MOR located within the nTS and the
94 subsequent hypoxia that develops after fentanyl exposure. Given that the majority of nTS MOR
95 is located on vagal afferent fibers, we utilized various techniques to evaluate opioid-induced
96 activity within the nTS and manipulate nTS MOR signaling during OIRD. Using wireless *in vivo*
97 fiber photometry, we show that fentanyl evokes a biphasic activity profile in nTS neurons,
98 characterized by a transient increase followed by a prolonged decrease in neuronal excitability.
99 NLXM pretreatment strongly attenuated this biphasic response, indicating that fentanyl-induced

nTS activity is influenced by MOR-expressing peripheral afferents. Together, these findings provide novel insights into peripheral mechanisms mediating OIRD and support peripheral MOR antagonism as a promising therapeutic strategy for managing OIRD for patients suffering from OUD while sparing the CNS-driven acute aversive behaviors that are observed with the use of NLX.

RESULTS

Intravenous fentanyl induces respiratory depression and activates nTS neurons in a dose-dependent manner

We first examined the effect of intravenous fentanyl to induce cardiorespiratory depression and activate neurons in the nucleus tractus solitarius (nTS). Catheterized rats received intravenous saline (1 ml/kg) or fentanyl at a range of doses (2, 20, or 50 µg/kg; **Figure 1A**), and cardiorespiratory parameters were measured up to 60 minutes. The first 20 minutes of these responses are shown in **Figure 1B-D**. As shown in **Table 1**, baseline cardiorespiratory parameters were similar between male and female rats that received 20 µg/kg fentanyl. There was a small but significant difference in basal heart rate in female rats that received 50 µg/kg fentanyl (**Table 2**). Neither saline nor 2 µg/kg fentanyl evoked a significant change in cardiorespiratory parameters. In comparison, both 20 and 50 µg/kg fentanyl produced rapid decreases in oxygen saturation, heart rate, and respiratory rate, with the largest decrease occurring after 50 µg/kg fentanyl. The nadir (defined as the lowest point measured after fentanyl) and recovery (calculated as 90% of baseline values prior to fentanyl) for each physiological parameter were assessed in all groups (**Figure 1E-J**). There was no significant difference in the nadir or recovery values between saline- and 2 µg/kg fentanyl-treated rats. In comparison, rats given 50 µg/kg fentanyl exhibited a significantly lower nadir in oxygen saturation (**Figure 1E**) and respiratory rate (**Figure 1I**) compared to 20 µg/kg. In addition, the recovery time was significantly longer in rats that received 50 µg/kg fentanyl compared to 20 µg/kg fentanyl (**Figure 1F,J)**. The nadir of bradycardia was similar between 20- and 50 µg/kg rats (**Figure 1G**), although the duration of the response was significantly longer in rats that received the highest dose of fentanyl (**Figure 1H**). Overall, we observed no sex differences in the nadir or recovery time in rats that received 20 µg/kg fentanyl. Female rats that received 50 µg/kg fentanyl exhibited a significantly longer recovery of respiratory rate, although oxygen saturation and heart rate recover times were similar to males (**Tables 3,4**). We next examined nTS activation (Fos-IR) following intravenous fentanyl (**Figure 1K)**. A significant increase in Fos-IR was observed after 2 µg/kg fentanyl, (**Figure 1L**), a dose that did not induce

134 cardiorespiratory depression. Further dose-dependent increases in Fos-IR were observed after
135 20 and 50 μg/kg fentanyl. We evaluated a subpopulation of catecholaminergic nTS neurons,
136 which are critical for full expression of hypoxia-evoked cardiorespiratory responses (*23*, *35*) for
137 activation after intravenous fentanyl (**Figure 1M**). These cells exhibited increased Fos-IR after 2
138 μg/kg fentanyl and were further activated at the highest dose of fentanyl (50 μg/kg).
139

140 **Peripheral opioid receptor antagonism prevents fentanyl-induced respiratory depression**

141 The above data provide a comprehensive assessment of the dose-dependent changes
142 in cardiorespiratory parameters and nTS neuronal activation evoked by intravenous fentanyl. To
143 gain insight into the extent to which central and peripheral opioid receptors mediate these
144 effects, separate cohorts of rats received intravenous administration of the centrally and
145 peripherally acting competitive opioid receptor antagonist naloxone (NLX; 1 mg/kg) or the
146 peripherally restricted opioid receptor antagonist naloxone methiodide (NLXM, 1 and 5 mg/kg).
147 Initial biodistribution experiments were performed to confirm the peripheral restriction of NLXM.
148 Catheterized rats that received intravenous NLXM (1 or 5 mg/kg) or NLX (1 mg/kg) were
149 evaluated for detection of NLX or NLXM in brain and plasma samples collected either 2 or 10
150 minutes after administration (**Figure 2A**). Neither dose of NLXM was detected within the central
151 nervous system at either time point evaluated (**Figure 2B,C**). Importantly, NLX was not detected
152 in these NLXM-treated groups. In comparison, rats that received intravenous NLX exhibited
153 significant, time-dependent detection of NLX in both plasma and brain samples (**Figure 2D**).
154 Thus our data are in agreement with previous reports confirming the peripheral restriction of
155 NLXM (*33*, *36*). We next evaluated cardiorespiratory changes from baseline in rats that received
156 intravenous NLX or NLXM at either dose (**Figure S3A**). Data indicate that neither NLX nor
157 NLXM significantly altered cardiorespiratory parameters from their baseline parameters (**Figure**
158 **S3E-J**). Based on these findings, we utilized NLXM to further investigate the roles of peripheral
159 MOR antagonism in the context of evaluating OIRD.

160 Catheterized rats received intravenous NLXM (1 or 5 mg/kg) or NLX (1 mg/kg) prior to
161 intravenous fentanyl administration at 20 μg/kg (**Figure 3A**) or 50 μg/kg (**Figure S1A**). As
162 shown in **Figure 3B-D and Figure S1B-D**, the responses evoked by 20 μg/kg and 50 μg/kg
163 fentanyl induced an onset and duration of cardiorespiratory depression that was similar to what
164 was observed in **Figure 1**. As expected, NLX pretreatment completely blocked the decrease in
165 cardiorespiratory parameters at both 20 μg/kg and 50 μg/kg doses of fentanyl. In rats that
166 received 20 μg/kg fentanyl, 1 mg/kg NLXM pretreatment prevented bradycardic and
167 hypoventilatory responses to fentanyl (**Figure 3B-D**). For all parameters, saline-pretreated rats

168 exhibited lower nadir values than NLX- and NLXM-pretreated rats, and there was no significant
169 difference in the nadir or duration between NLX (1 mg/kg) and NLXM (1 mg/kg) pretreated rats
170 that received 20 µg/kg fentanyl (**Figure 3E-J**). Although there was a small drop in the nadir of
171 oxygen saturation in NLXM-pretreated rats, this was not significantly different than NLX-
172 pretreated animals (**Figure 3E**, p=0.2292). In rats that received 50 µg/kg fentanyl, 1 mg/kg
173 NLXM pretreatment was unable to prevent the initial decrease in oxygen saturation and heart
174 rate (**Figure S1E,G**). However, the duration of these responses was significantly shorter
175 compared to saline-treated rats (**Figure S1F,H,J**). A higher dose of NLXM (5 mg/kg), which
176 does not cross the blood brain barrier (**Figure 2C**), was then used in a separate group of
177 animals that received 50 µg/kg fentanyl. Pretreatment with 5 mg/kg NLXM attenuated
178 cardiorespiratory depression. While the nadir of oxygen saturation was significantly lower than
179 NLX-pretreated rats, the duration of this effect was not significantly different between groups
180 (**Figure S1E-J**). No sex differences were observed in the nadir or recovery time of any
181 parameter (**Tables 3,4**). Together, these data demonstrate that peripheral MOR antagonism
182 can sufficiently prevent OIRD by 20 µg/kg fentanyl and strongly attenuates OIRD evoked by 50
183 µg/kg fentanyl.
184 Neuronal activation, as measured by Fos-IR, was examined in the nTS of rats pretreated
185 with saline or opioid receptor antagonists followed by 20 µg/kg (**Figure 3K**) or 50 µg/kg fentanyl
186 (**Figure S1K**). Saline pretreatment evoked the highest degree of fentanyl-induced Fos-IR in the
187 nTS, including in a subpopulation of TH-IR neurons. Blocking peripheral MOR signaling with
188 NLXM did not decrease fentanyl-induced nTS neuronal activation, while NLX, which blocks both
189 central and peripheral MORs, resulted in a significant reduction in nTS activation (**Figure 3L,M**).
190 In rats that received the highest dose of fentanyl, the number of nTS cells displaying Fos-IR was
191 similar between rats pretreated with saline and NLXM at both doses, with the only significant
192 reduction occurring in NLX-pretreated animals (**Figure S1L**). This degree of activation was also
193 observed in catecholaminergic cells (**Figure S1M**), although around 30% of TH-IR neurons also
194 displayed Fos-IR in NLX-pretreated rats.
195

196 **Peripheral opioid receptor antagonism reverses fentanyl-induced respiratory depression**
197 The above data demonstrate that peripheral MOR antagonism prevents fentanyl-induced
198 respiratory depression without affecting nTS neuronal activation as measured by Fos-IR. Given
199 that reversal of OIRD has more translational relevance, we next evaluated the extent to which
200 NLXM reverses cardiorespiratory depression after it has been induced by 20 µg/kg (**Figure 4A**)
201 or 50 µg/kg fentanyl (**Figure S2A**). Both 20 (**Figure 4B-D**) and 50 µg/kg fentanyl (**Figure S2B-**

202 **D**) induced rapid decreases in oxygen saturation, heart rate and respiratory rate, similar to what
203 was observed in **Figure 1**. The fentanyl-induced nadir in all physiological parameters prior to
204 intravenous administration of saline, NLX or NLXM was similar between groups. In rats that
205 received 20 µg/kg fentanyl, both intravenous NLX (1 mg/kg) and NLXM (1 mg/kg) restored
206 cardiorespiratory values to baseline significantly faster than saline-pretreated animals (**Figure**
207 **4F,H,J**). This reversal of cardiorespiratory parameters was similar between NLX- and NLXM-
208 treated animals. In rats that received 50 µg/kg fentanyl, NLX rapidly restored all physiological
209 parameters to their baseline values (**Figure S2F,H,J**). While 1 mg/kg NLXM did not sufficiently
210 reverse the OIRD induced by 50 µg/kg fentanyl (**Figure S2F**)**,** a higher dose of 5 mg/kg NLXM
211 fully reversed the fentanyl-induced bradycardia and hypoventilation. The time to restore
212 parameters to baseline was not significantly different than NLX. We did not observe any sex
213 differences in the nadir or recovery time of any parameter (**Tables 3,4**). Thus, blocking
214 peripheral MORs sufficiently reverses OIRD at both moderate and high doses of fentanyl.
215 Because acute hypoxia activates nTS neurons (*24*), we investigated the impact of
216 peripheral and central MOR antagonism on fentanyl-induced nTS neuronal activation (**Figure**
217 **4K**). At both doses of fentanyl administered, a similar degree of nTS neuronal activation was
218 observed in all groups regardless of MOR antagonist administered after fentanyl (**Figure 4L,M;**
219 **Figure S2L,M**). Together, these data demonstrate that selective antagonism of peripheral
220 opioid receptors sufficiently reverses cardiorespiratory depression induced by both moderate
221 and high doses of fentanyl. Moreover, these data suggest that even a brief period of fentanyl-
222 induced cardiorespiratory depression is sufficient to induce robust activation of nTS neurons,
223 and this subsequent MOR antagonism has no additional effect to increase nTS activation.
224
225 **Reversal of Fentanyl-Induced Respiratory Depression with NLXM is not aversive**
226 NLX rapidly reverses OIRD, but produces unwanted side effects including the immediate
227 onset of severe withdrawal (*12*, *13*). The intense symptoms induced during NLX-precipitated
228 withdrawal present additional challenges in managing OUD in patients. Given that peripheral
229 MOR antagonism sufficiently reverses fentanyl-induced cardiorespiratory depression to a
230 degree that is comparable to NLX, we used a conditioned place aversion (CPA) approach to
231 assess whether selective peripheral antagonism of MOR signaling produces aversive behaviors.
232 Rats underwent a 3-session CPA challenge that consisted of pre-conditioning test, conditioning
233 test, and post-conditioning test (**Figure 5A**). Horizontal locomotion in both compartments of the
234 CPA boxes was assessed during both pre- and post-conditioning tests (**Figure 5B**). During the
235 pre-conditioning test, rats exhibited no natural preference or aversion for either compartment.

236 On the conditioning day (Day 2), a divider was placed in the middle of the CPA box. Rats
237 received intravenous fentanyl (50 µg/kg) in their home cage. Four minutes later, rats were
238 placed into the paired compartment of the CPA box and immediately given intravenous saline (1
239 ml/kg), NLX (1 mg/kg) or NLXM (1 or 5 mg/kg). During the post-conditioning test, the divider
240 was removed, and rats were allowed to explore both compartments of the CPA box. **Figure 5C**
241 shows the time spent on the conditioned side of the CPA box for all groups. During the post-
242 conditioning test, NLX-treated animals spent significantly less time in the NLX-paired
243 compartment, suggesting that the reversal of OIRD on the conditioning day was aversive. This
244 conditioned place aversion behavior was not observed in rats that received NLXM at either dose
245 (**Figure 5D**). Importantly, a single conditioning session with fentanyl administered in the home
246 cage followed by saline in the compartment instead of a MOR antagonist did not produce a
247 preference or aversion to the saline-paired compartment. To rule out any potential effects of
248 endogenous opioids influencing the behavioral responses to opioid receptor antagonism, we
249 performed an additional test in which rats were given saline in their home cage, followed by NLX
250 or NLXM in one of the CPA compartments (**Figure 5E,F**). Neither antagonist produced a
251 preference nor aversion to the MOR antagonist-paired compartment (**Figure 5G**). There was no
252 difference in CPA scores between these groups (**Figure 5H**). These findings are consistent with
253 our data demonstrating that NLX and NLXM alone do not alter physiological parameters from
254 baseline (**Figure S3**).
255

256 **Fentanyl induces a biphasic activity profile in nTS neurons**

257 As shown in **Figure 1**, fentanyl induced robust Fos-IR expression in the nTS. While Fos-IR
258 quantification provides insight into the anatomical activation of brainstem subregions in
259 response to fentanyl administration and OIRD reversal, this approach does not provide any
260 temporal resolution of the activity of these cells. Therefore, we used wireless *in vivo* fiber
261 photometry to assess dynamic changes in nTS calcium transient activity after intravenous
262 fentanyl administration in anesthetized rats (**Figure 6A**). Catheterized rats underwent bilateral
263 injections of an AAV expressing a calcium sensor (pGP-AAV-syn-jGCaMP8m-WPRE) into the
264 nTS. On the day of the experiment, an optic fiber was lowered on the surface of the brainstem
265 above the nTS and calcium transient activity was recorded (**Figure 6B**). GCaMP viral
266 expression was observed throughout the caudal-rostral extent of the nTS in all rats (**Figure 6C**).
267 Fentanyl (20 µg/kg) infusion induced a biphasic activity profile in nTS neurons, characterized by
268 an initial robust increase (Early Response) followed by a decrease below baseline (Late
269 Response, **Figure 6D**). Pretreatment with NLXM (5 mg/kg) attenuated both phases of the

270 fentanyl-induced changes in neuronal activity. As shown in **Figure 6E**, the area under the curve
271 (AUC) was significantly elevated during the Early and Late Responses after fentanyl. In
272 contrast, no significant fentanyl-induced change in AUC was observed in NLXM-pretreated rats
273 at either time point, indicating that changes in fentanyl-induced nTS neuronal activity are
274 strongly mediated by peripheral MORs. We next examined the extent to which MOR antagonists
275 restore the fentanyl-induced reductions in activity. After MOR antagonist administration,
276 fentanyl-induced suppression of nTS activity returned to baseline during the early recovery in
277 rats that received NLX, but not NLXM. However, both NLX and NLXM enhanced nTS activity
278 above baseline during the late recovery period (**Figure 6F,G).** During the Late Recovery period,
279 nTS activity was significantly enhanced above baseline in both NLX and NLXM-treated animals.
280 Together, these data demonstrate that peripheral MOR antagonism is sufficient to reverse the
281 fentanyl-induced decrease in nTS neuronal activity.
282

283 # DISCUSSION

284 OIRD is a complex problem that continues to be at the forefront of the opioid epidemic
285 (*1*, *37*). The increased potency and faster onset of synthetic opioids like fentanyl has been
286 attributed to the rising wave of opioid-related deaths in the US (*2*, *11*). Numerous studies have
287 evaluated opioid-induced dysfunction within key regulatory sites in the central nervous system
288 that contribute to the severity of OIRD (*1*, *15*, *16*, *18*, *26*). Peripheral MORs have also been
289 examined for their roles in impacting OIRD (*12*, *34*). However, the specific contributions of
290 central and peripheral MORs to the onset and duration of fentanyl-induced cardiorespiratory
291 depression, along with the role of the nTS in these effects, are not completely understood. In
292 this study, we show that blocking peripheral MORs with NLXM sufficiently prevents and
293 reverses fentanyl-induced cardiorespiratory depression and systemic hypoxia. Furthermore, we
294 demonstrate that peripheral opioid receptors mediate fentanyl-induced activity of nTS neurons.
295 These data suggest that the nTS may be an area impacted by fentanyl via peripheral MOR
296 activation. Lastly, we demonstrate that in addition to reversing fentanyl-induced
297 cardiorespiratory depression, NLXM does not induce aversive behaviors, as compared to NLX.
298 Together, these findings provide evidence that peripheral MOR antagonism may be a potential
299 novel strategy to reverse OIRD without inducing withdrawal, anxiety, and aversion, all of which
300 can contribute to further relapse in drug-seeking behaviors (*2*, *13*).
301 While numerous studies have focused on evaluating the effects of opioids acting at
302 MORs present within brainstem and pontine networks, less attention has been given to

303 identifying peripheral MOR mechanisms contributing to OIRD. NLX is the most common
304 reversal agent used to treat OIRD (*13*, *37*). In addition to reversing opioid-induced analgesia,
305 NLX precipitates withdrawal symptoms and aversion in humans and rodents (*12*, *13*, *38*, *39*). In
306 this study, we demonstrate that NLX-mediated reversal of OIRD caused a conditioned place
307 aversion, as shown by a significant decrease in time spent in the NLX-associated compartment.
308 This is likely the result of the induction of withdrawal symptoms that occur following antagonism
309 of MOR in central reward pathways (*12*, *13*, *40*). In contrast, this aversive response was not
310 observed in rats that received NLXM. These data suggest that alleviating fentanyl-induced
311 respiratory distress without antagonizing central MOR may mitigate the aversive state produced
312 by NLX.
313 Conditioned place preference and aversion paradigms have been utilized to evaluate
314 rewarding and aversive properties of opioids and antagonists (*41–43*). Overall, we observed
315 relatively minimal sex differences in basal and fentanyl-induced changes in cardiorespiratory
316 depression, which is consistent with a previous report showing that sex differences due to
317 fentanyl are relatively minimal compared to other opioids such as heroin (*9*). Previous reports
318 have shown sexually dimorphic differences in fentanyl-induced conditioned place preference,
319 with higher doses of fentanyl affecting females only (*43*). In present study, we administered
320 fentanyl to male and female rats in the home cage followed by saline in the CPA box and
321 observed neither a preference nor aversion in either sex. This suggests that the results obtained
322 during OIRD-mediated reversal via NLX or NLXM are driven by effects within the CPA box and
323 are not influenced by the rewarding properties of fentanyl itself. While previous reports have
324 shown that NLX can be detected centrally after a subcutaneous injection of NLXM (*33*), we
325 observed no detectable amount of NLX or NLXM in brain tissue of rats that received intravenous
326 NLXM at either dose or time point. Our data demonstrate robust fentanyl-induced neuronal
327 activation in the nTS that appears to be mediated via peripheral MORs. Given the proximity of
328 the nTS to the circumventricular organ area postrema (*44*), this raises the possibility that
329 fentanyl can access the central nervous system via the area postrema to influence neuronal
330 activation. However, our data showing the lack of a conditioned place aversion following NLXM-
331 mediated reversal of OIRD support our biodistribution data showing no NLXM detection in brain
332 samples that the observed effects primarily involve fentanyl actions at MOR located in
333 peripheral sites. Similar to NLX, peripheral MOR antagonism with NLXM has been shown to
334 partially reverse opioid-induced analgesia (*12*, *45*) which may pose limitations for pain
335 management. While we report no changes in cardiorespiratory parameters from baseline
336 following intravenous administration of NLX or NLXM in drug-naïve animals, previous work has

337 shown that high doses of NLX elicit behavioral and physiological changes in humans, including
338 cognitive impairment, nausea, tachycardia and hypertension, even at low and moderate doses
339 (*14*, *46*, *47*). Future investigations are needed to evaluate mechanisms underlying the
340 therapeutic potential of NLXM as an intervention for managing OIRD in patients with OUDs.
341 The nTS is a region with a high degree of MOR expression, and appears to be primarily
342 located on afferent fibers arising from the vagus nerve (*7*, *25*, *48*). While MOR has been shown
343 to be present in nTS somas and dendrites (*25*, *26*), these MOR-expressing cells do not express
344 Fos following exposure to opioids or hypoxia (*26*), which suggests a mechanism of presynaptic
345 action of MOR signaling in the nTS. Likewise, the nodose ganglion (NG), which contains the cell
346 bodies of nTS-projecting vagal sensory afferents, has high expression of MOR (*32*), and intra-
347 nodose injection of fentanyl induces hypoventilation, although to a much lesser degree
348 compared to systemic fentanyl (*49*).
349 In the present study, we used fiber photometry to characterize nTS neuronal responses
350 to show that fentanyl induces an initial excitatory response in nTS cells. However, this response
351 was short-lasting compared to the subsequent decrease in activity below baseline, suggesting
352 that the primary effect of MOR signaling produce generalized inhibition of nTS neurons. This
353 prolonged suppression of nTS neuronal activity may contribute to the overall duration of OIRD.
354 Furthermore, our photometry data demonstrate that while the NLXM-mediated reversal of
355 fentanyl-induced inhibition of nTS neurons was slower compared to NLX, activity was eventually
356 restored. A similar finding was observed in OIRD experiments, as NLXM induced a rate of
357 recovery in all parameters that was comparable to NLX. Taken together, this suggests that
358 peripheral MOR antagonism may sufficiently override simultaneous central effects of fentanyl
359 acting at MOR present in cardiorespiratory nuclei, including the nTS.
360 It is important to note that while all our experiments assessing fentanyl-induced
361 cardiorespiratory depression were conducted in conscious rats breathing room air, photometry
362 experiments were performed under isoflurane anesthesia. Due to the location of the nTS,
363 chronic fiber implantation and subsequent in vivo photometry recordings in conscious,
364 unrestrained animals are not possible. In the nTS, Isoflurane has been reported to suppress
365 visceral afferent glutamatergic transmission and enhance GABAergic transmission via
366 postsynaptic mechanisms (*50*), as well as induce cFos expression in the nTS (*51*). Precautions
367 were taken to use the lowest dose of Isoflurane needed to maintain sufficient anesthesia.
368 However, we cannot rule out the possible influence of Isoflurane anesthesia to influence the
369 observed biphasic responses evoked by fentanyl. In addition, sex differences in physiological
370 and pharmacological responses to anesthesia have been previously described(*52*). Due to the

371 high attrition rate for these experiments, which require multiple survival surgeries and proper
372 fiber placement into the nTS, we were unable to fully evaluate potential sex differences and
373 cannot rule out the possibility of a sex effect of fentanyl-induced neural activity or in responses
374 to anesthesia. Nevertheless, our data support a mechanism by which fentanyl induces OIRD via
375 disruption of visceral afferent signaling to the nTS, thereby leading to prolonged OIRD due to
376 suppression of physiological reflex responses that would be normally engaged in response to
377 systemic hypoxia.

378 The nTS plays an essential role in the regulation of basal-and reflex-evoked
379 cardiorespiratory function (*22*). Activation of MOR in the nTS has been shown to blunt hypoxic
380 ventilatory responses following MOR agonism in the nTS (*7*). Our data are consistent with
381 previous work demonstrating opioid-induced activation of nTS neurons (*26*). The degree of
382 fentanyl induced Fos-IR in the nTS resembles what is observed after acute exposure to hypoxic
383 air (20, 46). Interestingly, we also observed increased Fos in the nTS at a dose of fentanyl that
384 was below the threshold to induce respiratory depression. It is unclear whether the Fos-IR
385 observed after low or high doses of fentanyl is, in part, the result of increased glutamatergic
386 transmission stemming from enhanced chemoreceptor afferent signaling to the nTS or via MOR
387 signaling within the nTS itself.

388 Glutamate is the primary neurotransmitter released from sensory afferent fibers into the
389 nTS (*22*, *53*). While intra-nTS application of opioid agonists have been shown to reduce
390 glutamate release and calcium channels via presynaptic mechanisms (*54*, *55*), opioids also
391 have been shown to induce a similar biphasic action of Ca2+-dependent spikes in the nodose
392 ganglion (*56*) that resembles what we observed in GCaMP-expressing nTS cells after
393 intravenous fentanyl. NLXM strongly attenuated the fentanyl-induced excitatory wave observed
394 in GCaMP-expressing nTS neurons, suggesting that MOR-expressing peripheral afferents
395 mediate this transient activation of nTS neurons, even if the primary effect of fentanyl is to inhibit
396 the nTS and suppress cardiorespiratory reflex function.

397 One possibility is that the increase in nTS activity may be mediated by opioid-induced
398 disinhibition within the nTS. The nTS contains a large population of second order GABAergic
399 interneurons that receive direct inputs from visceral afferents (*57*), and hypoxia activates these
400 cells(*23*). nTS MOR agonists suppress the activity of these cells, primarily via presynaptic
401 mechanisms (*58*), although postsynaptic mechanisms have been reported (*59*). Similarly,
402 visceral afferents also activate catecholaminergic nTS neurons (*60*), which are critical for the
403 generation of hypoxia-evoked cardiorespiratory responses(*35*, *61*). Opioids inhibit visceral
404 afferent transmission to this cell group, primarily via a presynaptic mechanism (*54*). In the

405 present study, we observed robust Fos expression in these cells at all doses of fentanyl
406 examined. These findings raise the possibility that nTS dysfunction, via MOR-expressing
407 peripheral inputs that terminate within this region, represents the first central site of fentanyl-
408 induced dysfunction, ultimately leading to downstream effects in other brain regions that
409 contribute to diminished autonomic and cardiorespiratory responses that contribute to the
410 duration of OIRD. Future studies are needed to fully evaluate the exact opioid-MOR effects in
411 the nTS, including specific MOR afferent inputs and the nTS phenotypes, to determine their
412 relative contributions to OIRD.
413 In summary, these studies highlight a significant involvement of peripheral MORs
414 contribute to the rapid cardiorespiratory depression induced by intravenous fentanyl. We have
415 provided extensive characterization into how fentanyl elicits cardiorespiratory depression and
416 examined the relationship between peripheral MORs and nTS activity in contributing to the
417 duration of OIRD. Moreover, our findings suggest that selectively blocking peripheral opioid
418 receptors could be a promising therapeutic strategy for managing OIRD. Notably, peripheral
419 opioid receptor antagonists are already prescribed for patients undergoing chemotherapy to
420 alleviate side effects such as opioid-induced constipation (*62*, *63*). Importantly, our data
421 demonstrate that peripheral MOR antagonism appears to reverse OIRD without triggering
422 unwanted effects of withdrawal that occur following NLX administration, suggesting that
423 peripheral MOR antagonists like NLXM could potentially be utilized in treatment strategies for
424 managing patients with OUD.

425 Materials and Methods:

426 All surgical and experimental procedures were approved by Washington University Committee
427 in accordance with the National Institutes of Health Guidelines for the Care and Use of
428 Laboratory Animals and Animal Research: Reporting In Vivo Experiments (ARRIVE) guidelines.
429 Rats were initially group-housed with two to three animals per cage on a 12/12-h dark/light cycle
430 (lights on at 7:00) and acclimated to the animal facility holding rooms for at least 7 days before
431 any manipulation. Following catheterization surgery, rats were single-housed and remained on
432 an identical 12/12-h dark/light cycle. The temperature for the holding rooms of all animals
433 ranged from 21 to 24 °C while the humidity was between 30 and 70%. Rats received food and
434 water ad libitum for the duration of all experiments. All experiments were performed during the
435 light cycle. For all experiments, male and female Sprague Dawley rats (250-350g) were used. In
436 all data sets, male rats are represented by filled symbols and female rats are represented by
437 open symbols.

438 **IV catheterization procedure:**
439 Animals were deeply anesthetized using Isoflurane (3% induction, 2% maintenance). A small
440 incision was made in the dorsal surface of the neck. Another small incision was made on the
441 ventral surface of the neck, and underlying tissue was carefully dissected to expose the jugular
442 vein. An indwelling catheter was inserted into the jugular vein and sutured in place using non-
443 absorbable silk suture. The catheter was then tunneled subcutaneously and exited the body
444 through the first small hole in neck on the dorsal side. The ventral incision was closed using
445 non-absorbable silk suture. The exposed catheter was connected to a backpack device
446 (Instech) containing a port for drug administration. Animals were given Carprofen (2 mg/kg sc),
447 Baytril (8 mg/kg sc) and bupivacaine (5 mg/kg, site of incision). In addition, rats were given
448 Carprofen tablets (Bio Serv, MD150-2) for 2 days after surgery to assist in wound healing and
449 analgesia. Rats were singly housed following surgery and were allowed to recover for one week
450 prior to the commencement of experiments. Catheter patency was maintained with daily flushing
451 of 0.3 mL sterile saline containing gentamicin (1.33 mg/mL, i.v.)

452 **Respiratory depression experiments:**
453 Following recovery from IV catheterization surgery, conscious, freely moving rats in their home
454 cages were fitted with a non-invasive pulse oximeter collar (Starr LifeSciences).
455 Cardiorespiratory parameters (oxygen saturation, heart rate and respiratory rate) were collected
456 (MouseOx v2.0, Starr LifeSciences) at baseline conditions in animals breathing room air, and
457 after intravenous administration of fentanyl citrate (2, 20 or 50 µg/kg). A subset of animals
458 received weight-adjusted intravenous administration of the nonselective opioid receptor
459 antagonist naloxone hydrochloride (NLX; 1 mg/kg; Sigma 51481-60-8) or the peripherally
460 restricted opioid receptor antagonist naloxone methiodide (NLXM; 1 or 5 mg/kg; Sigma N129)
461 before or after fentanyl administration. Cardiorespiratory parameters were then measured for up
462 to 60 minutes. For all OIRD experiments, the time course graphs consist of 30 seconds of data
463 averaged into a single data point. The nadir was defined as the lowest point measured after
464 fentanyl administration (for all graphs, red arrow indicates time of fentanyl administration,
465 time=0 minutes). In addition, the recovery rate was defined as the time to reach 90% baseline of
466 pre-fentanyl values for each cardiorespiratory parameter. Two hours after fentanyl
467 administration, rats were transcardially perfused with 0.01M PBS followed by paraformaldehyde
468 (4% in 0.01M PBS). Brains were removed and stored overnight at 4°C in 4% paraformaldehyde
469 for post-fixation, followed by at least 72 h incubation in sucrose (30% in 0.01M PBS) solution.
470 Isopentane was used to flash-freeze brains. Brainstem sections containing the nTS were sliced
471 in the coronal plane (40 µm) using a cryostat (Leica CM 1950).

472 **Biodistribution**

473 A subset of previously catheterized drug-naïve rats was deeply anesthetized and then received
474 intravenous administration of NLX (1 mg/kg) or NLXM (1 or 5 mg/kg). While still under
475 anesthesia, rats were quickly decapitated two or ten minutes after intravenous administration of
476 MOR antagonists. MOR antagonists were dosed in all rats at an experimentally relevant
477 concentration with triplicate blood and brain samples collected at two time points. The early time
478 point at 2 minutes evaluated conditions when the plasma concentration of the OR antagonist is
479 high and reflects the identical time point of intravenous administration for OIRD pretreatment
480 experiments. The second collection time point (10 minutes) was intended to evaluate steady-
481 state conditions and represent physiological experiments when reversal of OIRD was achieved
482 by both antagonists. Brains were quickly removed and flash frozen in liquid nitrogen. Trunk
483 blood was collected into capillary collection tubes containing lithium heparin (Greiner Bio-One;
484 Fisher Scientific). The blood was spun on a centrifuge for 10 min at 4 °C, and plasma was
485 carefully extracted from the supernatant. Brains and plasma samples underwent PK analyses
486 for detection of NLX or NLXM at both time points. Standard rat PK studies dosed the candidate
487 MOR antagonists and sample blood over multiple time points. A general description of tissue
488 distribution can be obtained during PK modeling by calculating the volume of distribution.
489 Samples underwent a direct measurement of peripheral restriction by measuring compound
490 concentration in plasma and brain.

491 **Conditioned Place Aversion**

492 The aversive effects following reversal of OIRD were measured using Conditioned Place
493 Aversion (CPA) (*64*). During a pre-conditioning session (Day 1), rats were allowed to explore
494 both sides of a two compartment CPA box for 15 minutes. On the Conditioning Day (Day 2), a
495 divider was placed in the middle of the box to restrict movement to one side on the box. Rats
496 were then randomly assigned to one side of the CPA box, and this side was paired with either
497 saline (1 ml/kg), NLX (1 mg/kg) or NLXM (1 or 5 mg/kg). Rats were given intravenous fentanyl
498 (50 µg/kg) or saline in their home cages. Four minutes later, they were placed in the paired side
499 of the box and immediately given saline or a MOR antagonist. Rats were confined to this
500 compartment for 15 minutes. For all CPA experiments, measures were taken to balance the
501 side of CPA box by drug and by sex. On the post-conditioning test (Day 3), the divider was
502 removed. Rats were then placed in the CPA box and allowed to explore both sides of the CPA
503 box for 15 minutes. The total time spent in the paired chamber and CPA scores were calculated
504 for all groups.

505 **Wireless *in vivo* Fiber Photometry**
506 To selectively measure nTS neuronal calcium transient activity, we injected an AAV containing a
507 calcium sensor expressed under the synapsin promoter (pGP-AAV-syn-jGCaMP8m-WPRE) into
508 the nTS (500 nl per side; 0.3-0.5 mm anterior, ± 0.4 mm lateral and 0.4 mm ventral to brain
509 surface, relative to calamus scriptorius). Rats were allowed at least 3 weeks to recover from
510 nanoinjection surgery to allow for robust viral expression in the nTS before IV catheters were
511 implanted as described above. On the day of the experiment, rats were deeply anesthetized
512 with isoflurane (3-4% induction, 2% maintenance), placed in the stereotaxic apparatus, and the
513 nTS was exposed as described above. To overcome limitations associated with chronic fiber
514 implants in the nTS, a wireless photometry headstage (TeleFipho, Amuza Inc.) was secured to
515 a 5 mm flat-tipped silica optic fiber cannula (400 μm c.d./470 μm o.d., NA 0.37, 2.5 mm
516 receptacle; Doric) and mounted the stereotaxic arm with an apparatus 3D printed in house to
517 permit simultaneous nTS exposure and photometry recordings. The optic fiber was lowered to
518 the site of the dorsal brainstem and firmly pressed on the surface above the nTS until a signal
519 was detected (~0.3-0.5 mm ventral from the surface). An LED generated blue light was
520 bandpass-filtered (445-490 nm) to excite jGCaMP8m and emission fluorescence was detected
521 by an internal photodiode detector for green light (bandpass filtered at 500-550 nm). An internal
522 DC amplifier transmitted the data (16-bit arbitrary unit; AU) to a wireless receiver (TeleFipho,
523 Amuza Inc.) and the data was extracted in real-time using TeleFipho software (Amuza Inc.) at a
524 sampling rate of 100 Hz. The offset was set to 90° and the LED power was adjusted to achieve
525 an optimal signal output (30-40k a.u.) not to exceed 36 mW power, and remained constant
526 throughout the recording. Baseline activity of GCaMP fluorescence nTS-infected cells was
527 measured after at least 5 min to mitigate effects of baseline drift in signal due to slow
528 photobleaching artifacts. Then, baseline activity was measured for at least 30 s prior to
529 administration of either fentanyl (20 μg/kg, i.v.) or NLXM (5 mg/kg, i.v.). After response activity
530 was recorded, rats received a second intravenous injection of either an opioid receptor
531 antagonist (NLX,1 mg/kg or NLXM, 5 mg/kg) or fentanyl (20 μg/kg), respectively. Each
532 intravenous administration was manually time locked to calcium transient recordings by a
533 second experimenter and response activity following each injection was recorded for 60 s
534 before administration of the second injection or conclusion of the experiment. Rats were
535 transcardially perfused with PFA at the end of the experiment as described above and viral
536 expression was validated for all animals.
537 For analysis of calcium transient activity, the raw data was fit to a double-exponential curve and
538 subtracted from the raw data to account for any residual effects of baseline drift. Matlab Signal

539 Analyzer was used to extract regions of interest (ROIs) in the signal in 90-s traces (30 s pre-
540 treatment, 60 s post-treatment) and traces were aligned to the time of injection. ROIs were
541 standardized as z-scores using the sample standard deviation, *S,* where $S = \sqrt{\frac{\sum_{i=1}^{n}(x_i - \bar{X})^2}{n-1}}$ such
542 that signals were centered to have a mean of 0 and scaled to have a standard deviation of 1.
543 Based on this, the area under the curve (AUC) of ROI z-scores were calculated in 30-s bins
544 using the trapezoidal rule (*trapz* function in Matlab) and one-sample t-tests were used to
545 determine differences relative to baseline (theoretical mean = 0). For presentation, transients
546 were down sampled by a factor of 10 with a phase offset of 2 and the resultant 10 Hz traces
547 were smoothed using a moving mean duration of 5% of total ROI.
548

549 **Immunohistochemistry (IHC):**

550 Immunohistochemical procedures were performed as previously described (*65*). Brainstem
551 sections containing the nTS were sliced using a cryostat (Leica) at a thickness of 40 um. Free-
552 floating sections were rinsed in 0.01M PBS, blocked in 10% Normal Donkey Serum (Sigma) in
553 0.01M PBS-triton, and then incubated with the following antibodies: cFos (Rabbit anti-cFos;
554 ab190289, Abcam; AB_2737414); Tyrosine Hydroxylase (TH, Mouse anti-TH; MAB318,
555 Millipore; AB_2201528). The following day, sections were rinsed with 0.01M PBS, incubated
556 with Donkey anti-Rabbit Cy3 and Donkey anti-Mouse Alexa fluor 488 (1:200; in 3% NDS and
557 0.3% Triton in 0.01M PBS) and used to visualize targets of interest (Jackson ImmunoResearch).

558 **Image acquisition:**

559 Immunoreactivity (IR) and viral expression were examined with a Leica DMR microscope at 20X
560 magnification. 20 µm thick z-stacks of the nTS (2 µm per plane) were collected. ImageJ (v. 1.48,
561 NIH) software was used for post-processing and analysis. In all groups, three sections of the
562 nTS (corresponding to -360, 0, +360 µm relative to calamus scriptorius) were collected.

563 **Brainstem immunohistochemical analyses**

564 Using ImageJ software, the regions containing the nTS were outlined, and unilateral counts of
565 Fos-IR, TH-IR and co-labeled Fos- and TH-IR neurons were performed using a custom-made
566 plugin (Cell Counter) for each of the 3 nTS sections per animal. The total number of each
567 phenotype was summed from these 3 sections, and the percentage of TH-IR cells co-
568 expressing Fos-IR was determined.

569 **Statistics**

570 For all experiments, the normality of sample data was determined using D'Agostino and
571 Pearson tests and Shapiro–Wilk tests. Statistical significance was taken as * $p<0.05$, ** $p<0.01$,
572 *** $p<0.001$ and ****$p<0.0001$, as determined by two-way repeated measures analysis of

variance (ANOVA) followed by Sidak's post hoc test; one-way ANOVA with Tukey post-hoc test, two-tailed unpaired t-test, two-tailed paired t-test, one sample t-test.

605 ## References

606 1. J.-M. Ramirez, N. J. Burgraff, A. D. Wei, N. A. Baertsch, A. G. Varga, H. A. Baghdoyan, R.
607 Lydic, K. F. Morris, D. C. Bolser, E. S. Levitt, Neuronal mechanisms underlying opioid-
608 induced respiratory depression: our current understanding. *Journal of Neurophysiology*
609 **125**, 1899–1919 (2021).

610 2. S. D. Comer, C. M. Cahill, Fentanyl: Receptor pharmacology, abuse potential, and
611 implications for treatment. *Neuroscience & Biobehavioral Reviews* **106**, 49–57 (2019).

612 3. C. L. Mattson, Trends and Geographic Patterns in Drug and Synthetic Opioid Overdose
613 Deaths — United States, 2013–2019. *MMWR Morb Mortal Wkly Rep* **70** (2021).

614 4. S. Parida, J. P. De Aquino, M. Sofuoglu, High potency synthetic opioids: Curbing the third
615 wave of the opioid crisis. *Neuroscience & Biobehavioral Reviews* **106**, 9–10 (2019).

616 5. N. Wilson, M. Kariisa, P. Seth, H. Smith, N. L. Davis, Drug and Opioid-Involved Overdose
617 Deaths — United States, 2017–2018. *MMWR Morb Mortal Wkly Rep* **69**, 290–297 (2020).

618 6. A. Mansour, C. A. Fox, S. Burke, F. Meng, R. C. Thompson, H. Akil, S. J. Watson, Mu,
619 delta, and kappa opioid receptor mRNA expression in the rat CNS: An in situ hybridization
620 study. *Journal of Comparative Neurology* **350**, 412–438 (1994).

621 7. J. Zhuang, X. Gao, F. Gao, F. Xu, Mu-opioid receptors in the caudomedial NTS are critical
622 for respiratory responses to stimulation of bronchopulmonary C-fibers and carotid body in
623 conscious rats. *Respir Physiol Neurobiol* **235**, 71–78 (2017).

624 8. R. Hill, R. Santhakumar, W. Dewey, E. Kelly, G. Henderson, Fentanyl depression of
625 respiration: Comparison with heroin and morphine. *Br J Pharmacol* **177**, 254–265 (2020).

626 9. R. C. N. Marchette, E. R. Carlson, E. V. Frye, L. E. Hastings, J. C. M. Vendruscolo, G.
627 Mejias-Torres, S. J. Lewis, A. Hampson, N. D. Volkow, L. F. Vendruscolo, G. F. Koob,
628 Heroin- and Fentanyl-Induced Respiratory Depression in a Rat Plethysmography Model:
629 Potency, Tolerance, and Sex Differences. *J Pharmacol Exp Ther* **385**, 117–134 (2023).

630 10. T. Lewanowitsch, R. J. Irvine, Naloxone and its quaternary derivative, naloxone
631 methiodide, have differing affinities for mu, delta, and kappa opioid receptors in mouse
632 brain homogenates. *Brain Res* **964**, 302–305 (2003).

633 11. N. Fairbairn, P. O. Coffin, A. Y. Walley, Naloxone for heroin, prescription opioid, and illicitly
634 made fentanyl overdoses: Challenges and innovations responding to a dynamic epidemic.
635 *International Journal of Drug Policy* **46**, 172–179 (2017).

636 12. T. Lewanowitsch, R. J. Irvine, Naloxone methiodide reverses opioid-induced respiratory
637 depression and analgesia without withdrawal. *European Journal of Pharmacology* **445**, 61–
638 67 (2002).

639 13. J. T. Lai, C. E. Goldfine, B. P. Chapman, M. M. Taylor, R. K. Rosen, S. P. Carreiro, K. M.
640 Babu, Nobody Wants to Be Narcan'd: A Pilot Qualitative Analysis of Drug Users'
641 Perspectives on Naloxone. *West J Emerg Med* **22**, 339–345 (2021).

642 14. B. Yugar, K. McManus, C. Ramdin, L. S. Nelson, M. A. Parris, Systematic Review of
643 Naloxone Dosing and Adverse Events in the Emergency Department. *The Journal of*
644 *Emergency Medicine* **65**, e188–e198 (2023).

645 15. I. Bachmutsky, X. P. Wei, E. Kish, K. Yackle, Opioids depress breathing through two small
646 brainstem sites. *eLife* **9**, e52694 (2020).

647 16. J. T. Bateman, E. S. Levitt, Opioid suppression of an excitatory pontomedullary respiratory
648 circuit by convergent mechanisms. *eLife* **12**, e81119 (2023).

649 17. A. Haji, H. Yamazaki, Y. Ohi, R. Takeda, Distribution of μ receptors in the ventral
650 respiratory group neurons; immunohistochemical and pharmacological studies in
651 decerebrate cats. *Neuroscience Letters* **351**, 37–40 (2003).

652 18. E. S. Levitt, A. P. Abdala, J. F. R. Paton, J. M. Bissonnette, J. T. Williams, μ opioid
653 receptor activation hyperpolarizes respiratory-controlling Kölliker–Fuse neurons and
654 suppresses post-inspiratory drive. *The Journal of Physiology* **593**, 4453–4469 (2015).

655 19. B. Palkovic, V. Marchenko, E. J. Zuperku, E. A. E. Stuth, A. G. Stucke, Multi-Level
656 Regulation of Opioid-Induced Respiratory Depression. *Physiology (Bethesda)* **35**, 391–404
657 (2020).

658 20. G. Montandon, W. Qin, H. Liu, J. Ren, J. J. Greer, R. L. Horner, PreBötzinger Complex
659 Neurokinin-1 Receptor-Expressing Neurons Mediate Opioid-Induced Respiratory
660 Depression. *J. Neurosci.* **31**, 1292–1301 (2011).

661 21. K. T. S. Pattinson, Opioids and the control of respiration. *British Journal of Anaesthesia*
662 **100**, 747–758 (2008).

663 22. M. C. Andresen, D. L. Kunze, Nucleus tractus solitarius--gateway to neural circulatory
664 control. *Annu Rev Physiol* **56**, 93–116 (1994).

665 23. T. L. King, C. M. Heesch, C. G. Clark, D. D. Kline, E. M. Hasser, Hypoxia activates nucleus
666 tractus solitarii neurons projecting to the paraventricular nucleus of the hypothalamus.
667 *American Journal of Physiology-Regulatory, Integrative and Comparative Physiology* **302**,
668 R1219–R1232 (2012).

669 24. L. J. Teppema, J. G. Veening, A. Kranenburg, A. Dahan, A. Berkenbosch, C. Olievier,
670 Expression of c-fos in the rat brainstem after exposure to hypoxia and to normoxic and
671 hyperoxic hypercapnia. *Journal of Comparative Neurology* **388**, 169–190 (1997).

672 25. S. A. Aicher, A. Goldberg, S. Sharma, V. M. Pickel, μ-opioid receptors are present in vagal
673 afferents and their dendritic targets in the medial nucleus tractus solitarius. *Journal of*
674 *Comparative Neurology* **422**, 181–190 (2000).

675 26. S. N. Maletz, B. T. Reid, A. G. Varga, E. S. Levitt, Nucleus Tractus Solitarius Neurons
676 Activated by Hypercapnia and Hypoxia Lack Mu Opioid Receptor Expression. *Front Mol*
677 *Neurosci* **15**, 932189 (2022).

678 27. A. Furdui, C. da Silveira Scarpellini, G. Montandon, Anatomical distribution of μ-opioid
679 receptors, neurokinin-1 receptors, and vesicular glutamate transporter 2 in the mouse
680 brainstem respiratory network. *Journal of Neurophysiology* **132**, 108–129 (2024).

681 28. A. Disney, K. M. Olson, A. M. Shafer, S. C. Moore, J. P. Anand, J. R. Traynor, S. M.
682 Husbands, Opioid Antagonists from the Orvinol Series as Potential Reversal Agents for
683 Opioid Overdose. *ACS Chem Neurosci* **13**, 3108–3117 (2022).

684 29. E. Solis, K. T. Cameron-Burr, Y. Shaham, E. A. Kiyatkin, Fentanyl-Induced Brain Hypoxia
685 Triggers Brain Hyperglycemia and Biphasic Changes in Brain Temperature.
686 *Neuropsychopharmacol.* **43**, 810–819 (2018).

687 30. E. Salas, E. Alonso, M. J. Polanco, M. V. Cano, M. Ruiz-Gayo, L. F. Alguacil, Differential
688 regulation of CDK5 and c-Fos expression by morphine in the brain of Lewis and Fischer
689 344 rat strains. *Neuroscience* **230**, 151–156 (2013).

690 31. P. J. Cabot, P. R. Dodd, T. Cramond, M. T. Smith, Characterization of non-conventional
691 opioid binding sites in rat and human lung. *Eur J Pharmacol* **268**, 247–255 (1994).

692 32. J.-L. Li, T. Kaneko, N. Mizuno, Effects of peripheral nerve ligation on expression of μ-
693 opioid receptor in sensory ganglion neurons: an immunohistochemical study in dorsal root
694 and nodose ganglion neurons of the rat. *Neuroscience Letters* **214**, 91–94 (1996).

695 33. D. Perekopskiy, A. Afzal, S. N. Jackson, L. Muller, A. S. Woods, E. A. Kiyatkin, The Role of
696 Peripheral Opioid Receptors in Triggering Heroin-induced Brain Hypoxia. *Sci Rep* **10**, 833
697 (2020).

698 34. F. Henderson Jr, W. J. May, R. B. Gruber, A. P. Young, L. A. Palmer, B. Gaston, S. J.
699 Lewis, Low-dose morphine elicits ventilatory excitant and depressant responses in
700 conscious rats: Role of peripheral μ-opioid receptors. *Open Journal of Molecular and*
701 *Integrative Physiology* **3**, 111–124 (2014).

702 35. T. L. King, B. C. Ruyle, D. D. Kline, C. M. Heesch, E. M. Hasser, Catecholaminergic
703 neurons projecting to the paraventricular nucleus of the hypothalamus are essential for
704 cardiorespiratory adjustments to hypoxia. *Am J Physiol Regul Integr Comp Physiol* **309**,
705 R721-731 (2015).

706 36. S. McGaraughty, P. Honore, C. T. Wismer, J. Mikusa, C. Z. Zhu, H. A. McDonald, B.
707 Bianchi, C. R. Faltynek, M. F. Jarvis, Endogenous opioid mechanisms partially mediate
708 P2X3/P2X2/3-related antinociception in rat models of inflammatory and chemogenic pain
709 but not neuropathic pain. *Br J Pharmacol* **146**, 180–188 (2005).

710 37. J. T. Bateman, S. E. Saunders, E. S. Levitt, Understanding and countering opioid-induced
711 respiratory depression. *British Journal of Pharmacology* **n/a** (2021).

712 38. J. Neale, J. Strang, Naloxone—does over-antagonism matter? Evidence of iatrogenic harm
713 after emergency treatment of heroin/opioid overdose. *Addiction* **110**, 1644–1652 (2015).

714 39. A. Dahan, R. van der Schrier, T. Smith, L. Aarts, M. van Velzen, M. Niesters, Averting
715 Opioid-induced Respiratory Depression without Affecting Analgesia. *Anesthesiology* **128**,
716 1027–1037 (2018).

717 40. M. J. Katovich, J. W. Simpkins, J. O'Meara, Effects of opiod antagonists and their
718 quaternary analogs on temperature changes in morphine-dependent rats. *Life Sciences*
719 **39**, 1845–1854 (1986).

720 41. J. M. Finlay, A. Jakubovic, A. G. Phillips, H. C. Fibiger, Fentanyl-induced conditional place
721 preference: lack of associated conditional neurochemical events. *Psychopharmacology*
722 *(Berl)* **96**, 534–540 (1988).

723 42. A. D. Gaulden, N. Burson, N. Sadik, I. Ghosh, S. J. Khan, S. Brummelte, S. Kallakuri, S. A.
724 Perrine, Effects of fentanyl on acute locomotor activity, behavioral sensitization, and
725 contextual reward in female and male rats. *Drug Alcohol Depend* **229**, 109101 (2021).

726 43. Z. T. Knauss, C. J. Hearn, N. C. Hendryx, F. S. Aboalrob, Y. Mueller-Figueroa, D. S.
727 Damron, S. J. Lewis, D. Mueller, Fentanyl-induced reward seeking is sex and dose
728 dependent and is prevented by D-cysteine ethylester. *Front. Pharmacol.* **14** (2023).

729 44. C. J. Price, T. D. Hoyda, A. V. Ferguson, The area postrema: a brain monitor and
730 integrator of systemic autonomic state. *Neuroscientist* **14**, 182–194 (2008).

731 45. V. Spahn, G. Del Vecchio, D. Labuz, A. Rodriguez-Gaztelumendi, N. Massaly, J. Temp, V.
732 Durmaz, P. Sabri, M. Reidelbach, H. Machelska, M. Weber, C. Stein, A nontoxic pain killer
733 designed by modeling of pathological receptor conformations. *Science* **355**, 966–969
734 (2017).

735 46. MartinR. Cohen, RobertM. Cohen, D. Pickar, H. Weingartner, DennisL. Murphy, WilliamE.
736 Bunney, Behavioural effects after high dose naloxone administration to normal volunteers.
737 *The Lancet* **318**, 1110 (1981).

738 47. M. R. Cohen, R. M. Cohen, D. Pickar, D. L. Murphy, W. E. Bunney, Physiological effects of
739 high dose naloxone administration to normal adults. *Life Sci* **30**, 2025–2031 (1982).

740 48. S. Nomura, Y.-Q. Ding, T. Kaneko, J.-L. Li, N. Mizuno, Localization of μ-opioid receptor-
741 like immunoreactivity in the central components of the vagus nerve: A light and electron
742 microscope study in the rat. *Neuroscience* **73**, 277–286 (1996).

743 49. Z. Zhang, C. Zhang, M. Zhou, F. Xu, Activation of Opioid μ-Receptors, but not δ- or κ-
744 Receptors, Switches Pulmonary C-Fiber-Mediated Rapid Shallow Breathing into An Apnea
745 in Anesthetized Rats. *Respir Physiol Neurobiol* **183**, 211–217 (2012).

746 50. J. H. Peters, S. J. McDougall, D. Mendelowitz, D. R. Koop, M. C. Andresen, Isoflurane
747 Differentially Modulates Inhibitory and Excitatory Synaptic Transmission to the Solitary
748 Tract Nucleus. *Anesthesiology* **108**, 675–683 (2008).

749 51. Y. Hu, J. T. Qi, Z. Zhang, M. Q. Luo, Y. W. Wang, Comparative Brain-Wide Mapping of
750 Isoflurane and Ketamine-Activated Nuclei and Functional Networks. *eLife* **12** (2023).

751 52. L. J. Mawhinney, D. Mabourakh, M. C. Lewis, Gender-Specific Differences in the Central
752 Nervous System's Response to Anesthesia. *Transl. Stroke Res.* **4**, 462–475 (2013).

753 53. W. T. Talman, M. H. Perrone, D. J. Reis, Evidence for L-glutamate as the neurotransmitter
754 of baroreceptor afferent nerve fibers. *Science* **209**, 813–815 (1980).

755 54. R. J. Cui, B. L. Roberts, H. Zhao, M. C. Andresen, S. M. Appleyard, Opioids inhibit visceral
756 afferent activation of catecholamine neurons in the solitary tract nucleus. *Neuroscience*
757 **222**, 181–190 (2012).

758 55. H. Rhim, R. J. Miller, Opioid receptors modulate diverse types of calcium channels in the
759 nucleus tractus solitarius of the rat. *J. Neurosci.* **14**, 7608–7615 (1994).

760 56. H. Higashi, P. Shinnick-Gallagher, J. P. Gallagher, Morphine enhances and depresses
761 Ca2+-dependent responses in visceral primary afferent neurons. *Brain Research* **251**,
762 186–191 (1982).

763 57. T. W. Bailey, S. M. Appleyard, Y.-H. Jin, M. C. Andresen, Organization and properties of
764 GABAergic neurons in solitary tract nucleus (NTS). *J Neurophysiol* **99**, 1712–1722 (2008).

765 58. A. J. Boxwell, Y. Yanagawa, S. P. Travers, J. B. Travers, The μ-opioid receptor agonist
766 DAMGO presynaptically suppresses solitary tract-evoked input to neurons in the rostral
767 solitary nucleus. *J Neurophysiol* **109**, 2815–2826 (2013).

768 59. N. R. Glatzer, B. N. Smith, Modulation of synaptic transmission in the rat nucleus of the
769 solitary tract by endomorphin-1. *J Neurophysiol* **93**, 2530–2540 (2005).

770 60. S. M. Appleyard, D. Marks, K. Kobayashi, H. Okano, M. J. Low, M. C. Andresen, Visceral
771 afferents directly activate catecholamine neurons in the solitary tract nucleus. *J Neurosci*
772 **27**, 13292–13302 (2007).

773 61. C. S. Bathina, A. Rajulapati, M. Franzke, K. Yamamoto, J. T. Cunningham, S. Mifflin,
774 Knockdown of tyrosine hydroxylase in the nucleus of the solitary tract reduces elevated
775 blood pressure during chronic intermittent hypoxia. *Am J Physiol Regul Integr Comp*
776 *Physiol* **305**, R1031–R1039 (2013).

777 62. E. Floettmann, K. Bui, M. Sostek, K. Payza, M. Eldon, Pharmacologic Profile of Naloxegol,
778 a Peripherally Acting μ-Opioid Receptor Antagonist, for the Treatment of Opioid-Induced
779 Constipation. *J Pharmacol Exp Ther* **361**, 280–291 (2017).

780 63. J. V. Pergolizzi, P. J. Christo, J. A. LeQuang, P. Magnusson, The Use of Peripheral μ-
781 Opioid Receptor Antagonists (PAMORA) in the Management of Opioid-Induced
782 Constipation: An Update on Their Efficacy and Safety. *Drug Des Devel Ther* **14**, 1009–
783 1025 (2020).

784 64. T. M. Tzschentke, Measuring reward with the conditioned place preference (CPP)
785 paradigm: update of the last decade. *Addict Biol* **12**, 227–462 (2007).

786 65. B. C. Ruyle, D. Martinez, C. M. Heesch, D. D. Kline, E. M. Hasser, The PVN enhances
787 cardiorespiratory responses to acute hypoxia via input to the nTS. *Am J Physiol Regul*
788 *Integr Comp Physiol* **317**, R818–R833 (2019).

Acknowledgements

We wish to thank Justin Meyer for breeding the rat colonies that were used in these experiments and for general assistance throughout the experiments. We also thank Mike Cameron (Scripps Institute) for mass spectrometry experiments used for all biodistribution experiments. We also wish to thank Kristine Yoon and Thomas Schodl for their technical assistance.

Author Contributions

Conceptualization: BCR NM and JAM

Methodology: BCR, NM and JAM

Formal analysis of all data: BCR, SM, RK, MT and JAH

Photometry acquisition and extraction: BCR and JAH

Respiratory depression experiments: BCR, SM, RK, MT, JM, CGR, SAL

Conditioned Place Aversion: BCR, SM, MT, JM

Biodistribution experiments: BCR and TL

Immunohistochemistry, microscopy and cell counting: BCR, SM, RK, MT, JM, SAL

Catheterization surgeries: BCR, SM, RK, MT, JM, SAL

Writing of original draft: BCR

Writing (review and editing): BCR, RK, JM, SAL, TL, JAH, NM, JAM

Funding Acquisition, BCR, JAM

Resources: JAM

Supervision: BCR and JAM

Data Availability Statement

The authors confirm that all relevant data are included in the paper and its Supplementary Information files. All data generated in this study are provided in the Supplementary

Information/Source Data file. Further information and requests for resources and reagents should be directed to and will be fulfilled by the Lead Contact, Jose A. Morón (jmoron-concepcion @wustl.edu).

Competing Interests

We have no competing interests to declare.

Funding:

National Institute of Health grant R01DA042499 (JMC)

National Institute of Health grant R01DA045463 (JMC)

National Institute of Health grant R01DA054900(JMC)

National Institute of Health grant R56DA059067 (JMC)

Washington University McDonnell Small Grants Program GF0012452 (BCR)

National Institute of Health grant T32DA007261 (BCR)

National Institute of Health grant S10OD030332-01(Michael Cameron, Scripps Research)

FIGURES

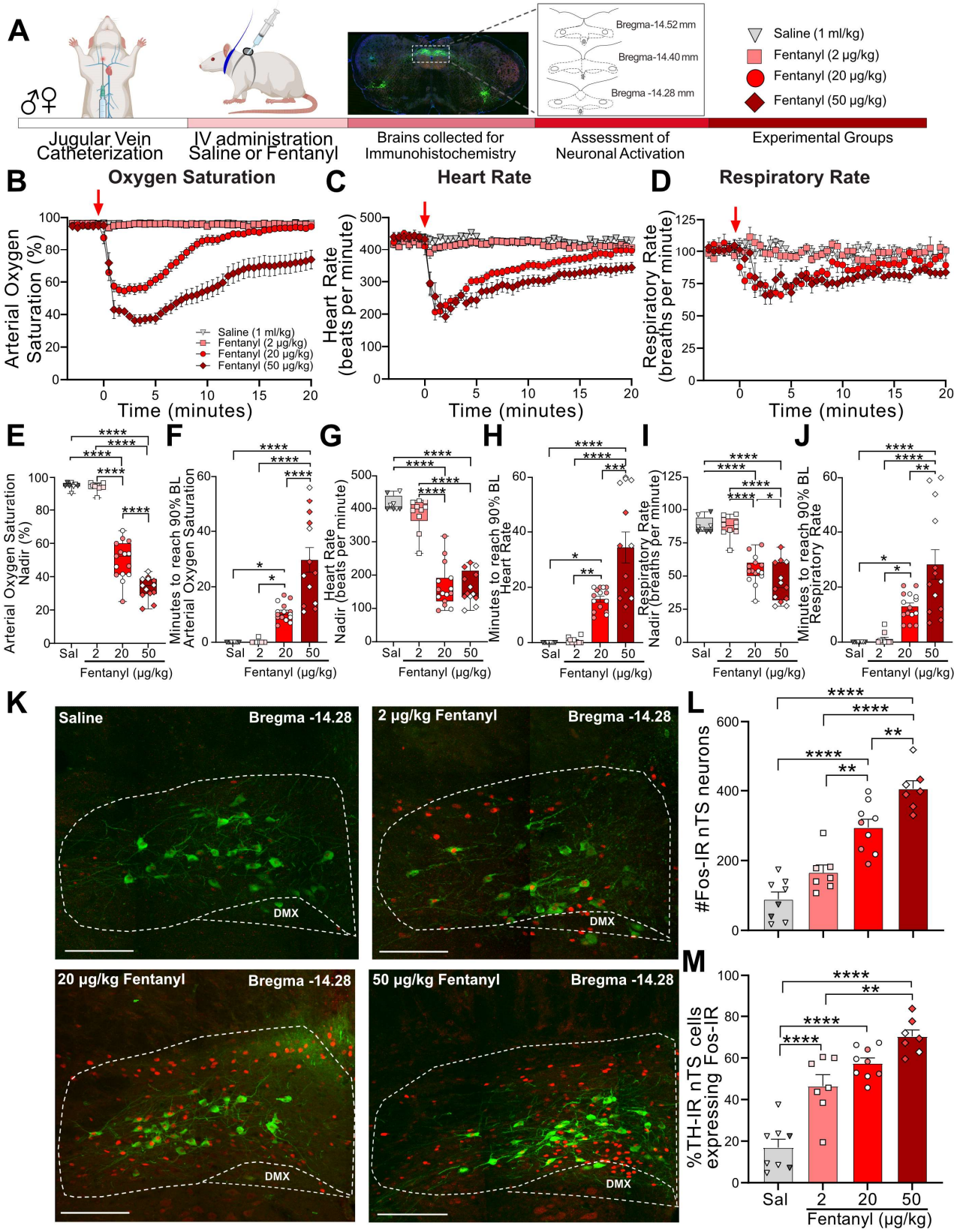
A
Bregma-14.52 mm
Bregma-14.40 mm
Bregma -14.28 mm
Saline (1 ml/kg)
Fentanyl (2 µg/kg)
Fentanyl (20 µg/kg)
Fentanyl (50 µg/kg)
Jugular Vein Catheterization
IV administration Saline or Fentanyl
Brains collected for Immunohistochemistry
Assessment of Neuronal Activation
Experimental Groups
B Oxygen Saturation
Arterial Oxygen Saturation (%)
Time (minutes)
C Heart Rate
Heart Rate (beats per minute)
D Respiratory Rate
Respiratory Rate (breaths per minute)
E
Arterial Oxygen Saturation Nadir (%)
F
Minutes to reach 90% BL Arterial Oxygen Saturation
G
Heart Rate Nadir (beats per minute)
H
Minutes to reach 90% BL Heart Rate
I
Respiratory Rate Nadir (breaths per minute)
J
Minutes to reach 90% BL Respiratory Rate
Sal
Fentanyl (µg/kg)
K
Saline
2 µg/kg Fentanyl
20 µg/kg Fentanyl
50 µg/kg Fentanyl
Bregma -14.28
DMX
L
#Fos-IR nTS neurons
M
%TH-IR nTS cells expressing Fos-IR

831 **Figure 1: Fentanyl induces cardiorespiratory depression and nTS neuronal activation in a**
832 **dose-dependent manner**
833 **A.** Schematic showing the timeline for OIRD collar experiments. Male and Female SD rats
834 underwent jugular catheterization surgery. One week later, conscious rats in their home cages
835 were fitted with a pulse oximeter collar and received intravenous administration of either saline
836 (n=8, triangles) or fentanyl at doses of 2 µg/kg (n=10, squares), 20 µg/kg (n=15, circles), or 50
837 µg/kg (n=13, diamonds). In all graphs, males are represented by filled symbols, and females by
838 open symbols. Baseline cardiorespiratory parameters were measured for 3 minutes prior to
839 intravenous administration and up to 60 minutes after saline or fentanyl. At the conclusion of
840 experiments, brains were collected from a subset of animals in each group and processed for
841 Fos- and TH- immunoreactivity. Time course data showing oxygen saturation (**B**), heart rate (**C**)
842 and respiratory rate (**D**) data measurements in all groups before and after saline or fentanyl.
843 Changes in oxygen saturation were assessed as nadir (lowest value; **E,G,I**) and time to recover
844 to 90% of baseline (pre-saline/fentanyl; **F,H,J**) administration. There was a dose-dependent
845 decrease in the nadir for oxygen saturation (One-way ANOVA, $F_{(3,42)} = 186.3$, $p < 0.0001$;
846 Tukey's post-hoc ****p<0.0001), heart rate (One-way ANOVA $F_{(3, 42)} = 74.93$, $p < 0.0001$;
847 Tukey's post-hoc ****p<0.0001) and respiratory rate (One-way ANOVA, $F_{(3, 42)} = 45.60$, p
848 <0.0001; Tukey's post-hoc ****p<0.0001, *p<0.05). Time to recover to 90% baseline Oxygen
849 Saturation (One-way ANOVA, $F_{(3, 42)} = 28.72$, $p < 0.0001$; Tukey's post-hoc ****p<0.0001,
850 *p<0.05) heart rate (One-way ANOVA, $F_{(3, 42)} = 23.89$, $p < 0.0001$; Tukey's post-hoc
851 ****p<0.0001, ***p<0.001, **p<0.01, *p<0.05) and respiratory rate (One-way ANOVA, $F_{(3, 42)}$ =
852 16.53, p<0.0001; Tukey's post-hoc ****p<0.0001, **p<0.01, *p<0.05). **K.** Merged
853 photomicrographs of coronal brainstem sections displaying representative Fos- and TH-
854 immunoreactivity in the nTS of rats that received intravenous saline or fentanyl. Scale bar = 200
855 µm. **L.** Mean data show that 20 and 50 µg/kg fentanyl induced a significantly greater number of
856 Fos-IR cells in the nTS compared to saline and 2 µg/kg fentanyl. (One-way ANOVA, $F_{(3,27)}$ =
857 37.13, $p < 0.0001$; Tukey's post hoc ****p<0.0001, **p<0.001) **M.** Mean data showing the
858 percentage of TH-IR nTS neurons expressing Fos-IR. Rats that received 2 µg/kg fentanyl
859 displayed a significantly higher increase in activated TH-IR neurons compared to saline-treated
860 rats. Both 20 and 50 µg/kg fentanyl induced a significantly higher percentage of activation in
861 TH-IR cells compared to saline and 2 µg/kg fentanyl. (One-way ANOVA, $F_{(3,27)} = 37.13$,
862 p<0.0001; Tukey's post-hoc ****p<0.0001, **p<0.01)

863

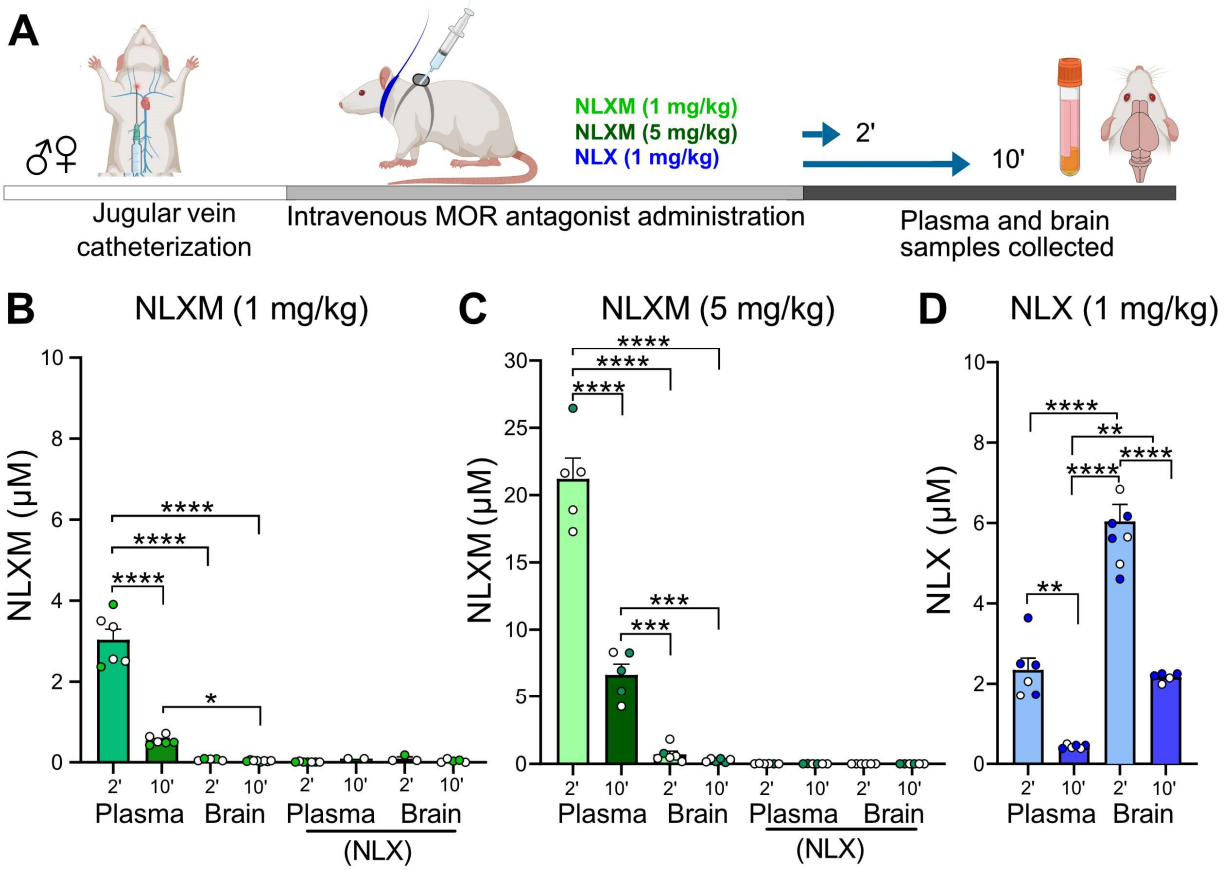
A
♂♀
NLXM (1 mg/kg)
NLXM (5 mg/kg)
NLX (1 mg/kg)
2'
10'
Jugular vein catheterization
Intravenous MOR antagonist administration
Plasma and brain samples collected
B
NLXM (1 mg/kg)
NLXM (μM)
C
NLXM (5 mg/kg)
NLXM (μM)
D
NLX (1 mg/kg)
NLX (μM)
2' 10' 2' 10' 2' 10' 2' 10'
Plasma Brain Plasma Brain
(NLX)

871 **Figure 2: NLXM does not cross the blood brain barrier**. **A**. Timeline of biodistribution
872 experiments. Male and female SD rats underwent intravenous jugular catheterization surgery.
873 The following week, rats were anesthetized and received intravenous NLXM (1 or 5 mg/kg) or
874 NLX (1 mg/kg). Rats were sacrificed 2 and 10 minutes after intravenous administration of MOR
875 antagonists. Plasma was extracted from trunk blood and intact brains were removed and rapidly
876 frozen with liquid nitrogen. **B**. Amount of NLXM detected in plasma and brain samples at each
877 time point after intravenous NLXM (1 mg/kg). One-way ANOVA, $F_{(3,21)} = 125.6$, $p < 0.0001$;
878 Tukey's post-hoc test, **** $p<0.0001$; * $p<0.05$. No NLX formation was detected in these
879 samples. **C**. Amount of NLXM detected in plasma and brain samples at each time point after
880 intravenous NLXM (5 mg/kg). One-way ANOVA, $F_{(3,18)} = 144.0$, $p < 0.0001$; Tukey's post-hoc
881 test, **** $p<0.0001$; *** $p<0.001$. No NLX formation was detected in these samples. **D**. Amount
882 of NLX detected in plasma and brain samples at each time point after intravenous NLX (1
883 mg/kg). One-way ANOVA, $F_{(3,21)} = 66.05$, $p < 0.0001$; Tukey's post-hoc test, **** $p<0.0001$; **
884 $p<0.01$.

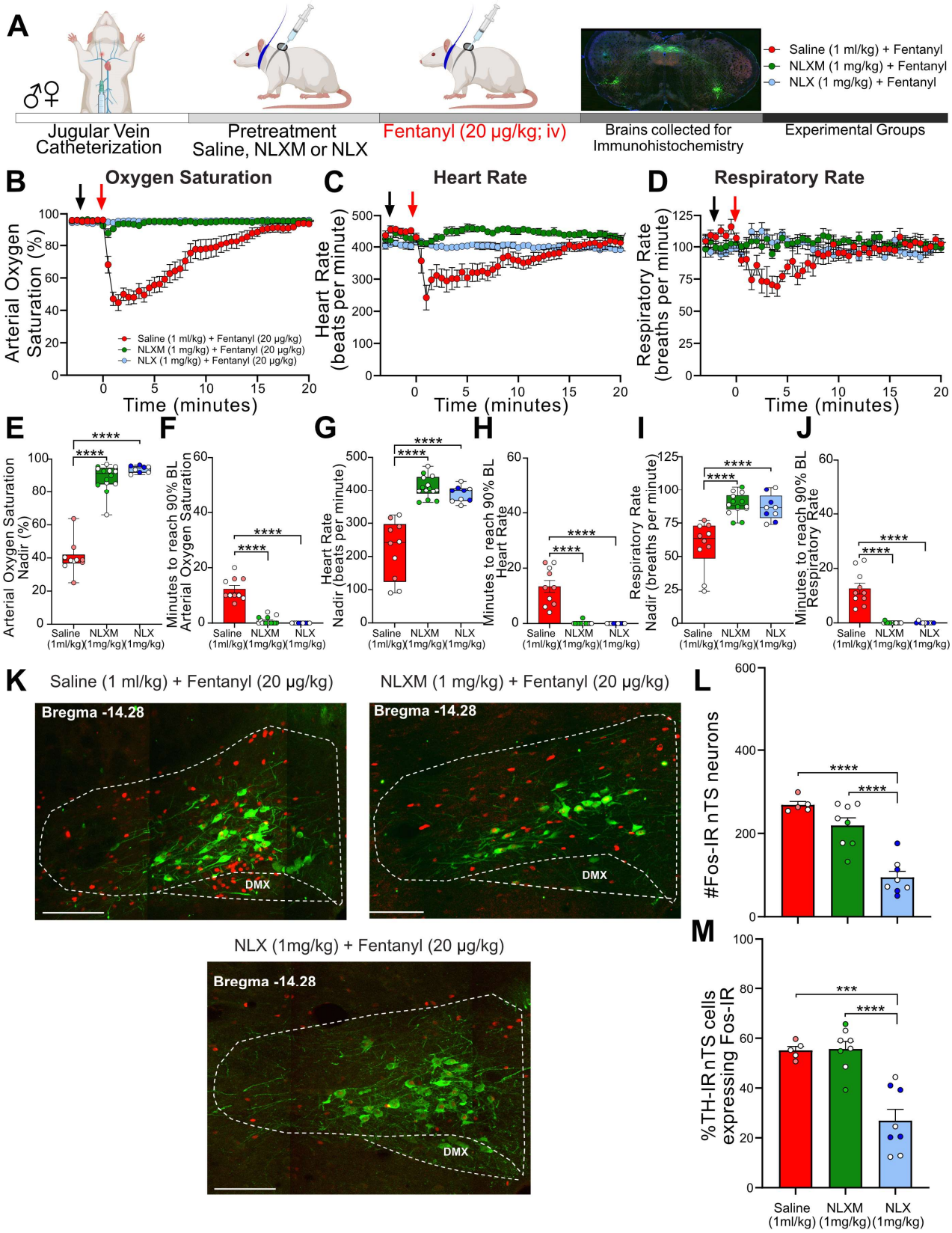
A
♂♀
Jugular Vein Catheterization
Pretreatment Saline, NLXM or NLX
Fentanyl (20 µg/kg; iv)
Brains collected for Immunohistochemistry
Experimental Groups
Saline (1 ml/kg) + Fentanyl
NLXM (1 mg/kg) + Fentanyl
NLX (1 mg/kg) + Fentanyl
B Oxygen Saturation
Arterial Oxygen Saturation (%)
Saline (1 ml/kg) + Fentanyl (20 µg/kg)
NLXM (1 mg/kg) + Fentanyl (20 µg/kg)
NLX (1 mg/kg) + Fentanyl (20 µg/kg)
Time (minutes)
C Heart Rate
Heart Rate (beats per minute)
Time (minutes)
D Respiratory Rate
Respiratory Rate (breaths per minute)
Time (minutes)
E
Arterial Oxygen Saturation Nadir (%)
F
Minutes to reach 90% BL Arterial Oxygen Saturation
G
Heart Rate Nadir (beats per minute)
H
Minutes to reach 90% BL Heart Rate
I
Respiratory Rate Nadir (breaths per minute)
J
Minutes to reach 90% BL Respiratory Rate
Saline (1ml/kg)
NLXM (1mg/kg)
NLX (1mg/kg)
K
Saline (1 ml/kg) + Fentanyl (20 µg/kg)
NLXM (1 mg/kg) + Fentanyl (20 µg/kg)
NLX (1mg/kg) + Fentanyl (20 µg/kg)
Bregma -14.28
DMX
L
#Fos-IR nTS neurons
M
%TH-IR nTS cells expressing Fos-IR

885

886 **Figure 3. NLXM attenuates respiratory depression without altering nTS Fos-IR induced by**
887 **20 µg/kg fentanyl: A.** Schematic showing the timeline for OIRD collar experiments. Male and
888 Female SD rats underwent jugular catheterization surgery. The following week, conscious rats
889 in their home cages received intravenous administration (pretreatment) of either saline (1 ml/kg;
890 n=10), NLX (1 mg/kg; n=9) or NLXM (1 mg/kg; n=15). Two minutes later, all rats received
891 intravenous fentanyl (20 µg/kg). Cardiorespiratory parameters were measured up to 60 minutes
892 after fentanyl. At the conclusion of the experiment, brains were collected from a subset of
893 animals in each group and processed for Fos- and TH- immunoreactivity. Time course data
894 showing oxygen saturation (**B**), heart rate (**C**) and respiratory rate (**D**) data measurements
895 collected in all groups before and after saline, NLX or NLXM pretreatment and after fentanyl.
896 Changes in oxygen saturation were assessed as nadir (lowest value after fentanyl; **E,G,I**) and
897 time to recover to 90% of baseline (**F,H,J**). In all graphs, males are represented by filled
898 symbols, and females by open symbols. Mean nadir values were assessed in saline-, NLX- and
899 NLXM-pretreated rats (Oxygen Saturation: One-way ANOVA, $F_{(2,30)} = 152.0$, $p<0.0001$; Tukey's
900 post-hoc test, ****$p<0.0001$; Heart Rate: One-way ANOVA, $F_{(2,30)} = 38.58$, $p<0.0001$; Tukey's
901 post-hoc test, ****$p<0.0001$; Respiratory Rate: One-way ANOVA, $F_{(2,30)} = 20.16$, $p<0.0001$;
902 Tukey's post-hoc test, ****$p<0.0001$). Time to reach 90% baseline in saline-, NLX- and NLXM-
903 pretreated rats. Mean time to reach 90% baseline was assessed for all parameters. Oxygen
904 Saturation: (One-way ANOVA, $F_{(2,30)} = 81.9$, $p<0.0001$; Tukey's post-hoc test ****$p<0.0001$;
905 Heart rate: (One-way ANOVA, $F_{(2,30)} = 44.11$, $p<0.0001$; Tukey's post-hoc test ****$p<0.0001$);
906 Respiratory rate: (One-way ANOVA, $F_{(2,30)} = 46.74$, $p<0.0001$; Tukey's post-hoc test
907 ****$p<0.0001$). **K.** Merged photomicrographs of a coronal brainstem section showing
908 representative Fos- and TH- immunoreactivity in the nTS of rats that received fentanyl with or
909 without saline or NLX/NLXM pretreatment. Scale bar = 200 µm. Fos-IR and the percentage of
910 TH-IR neurons expressing Fos-IR was evaluated in 3 nTS sections per rat. **L.** Mean data show
911 no significant difference in the number of Fos-IR cells between saline- and NLXM-pretreated
912 rats. NLX-pretreated rats displayed the lowest degree of Fos-IR in the nTS. Number of Fos-IR
913 cells: One-way ANOVA, $F_{(2,18)} = 30.52$, $p<0.0001$; Tukey's post-hoc ****$p<0.0001$. **M.** Mean data
914 of the percentage of TH-IR nTS cells expressing Fos-IR. The percentage of TH-IR cells
915 expressing Fos-IR was similar between saline- and NLXM-pretreated rats. NLX-pretreated rats
916 displayed the lowest percentage of Fos-IR in TH-IR nTS cells. Fos+TH/TH: (One-way ANOVA,
917 $F_{(2,18)} = 21.33$, $p<0.0001$; Tukey's post-hoc ****$p<0.0001$; ***$p<0.001$).

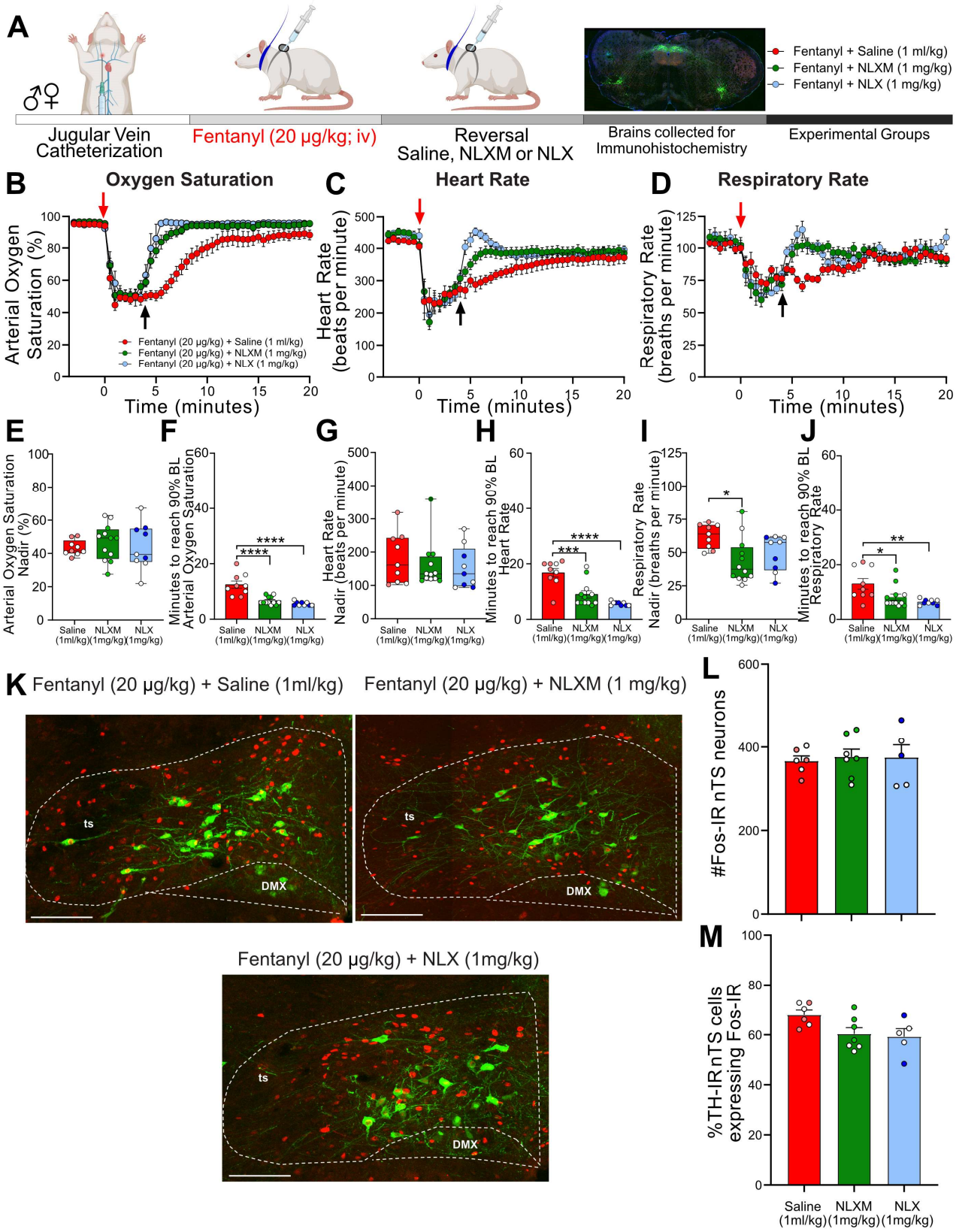
A
♂♀
Jugular Vein Catheterization
Fentanyl (20 µg/kg; iv)
Reversal Saline, NLXM or NLX
Brains collected for Immunohistochemistry
Experimental Groups
Fentanyl + Saline (1 ml/kg)
Fentanyl + NLXM (1 mg/kg)
Fentanyl + NLX (1 mg/kg)
B Oxygen Saturation
Arterial Oxygen Saturation (%)
Time (minutes)
Fentanyl (20 µg/kg) + Saline (1 ml/kg)
Fentanyl (20 µg/kg) + NLXM (1 mg/kg)
Fentanyl (20 µg/kg) + NLX (1 mg/kg)
C Heart Rate
Heart Rate (beats per minute)
D Respiratory Rate
Respiratory Rate (breaths per minute)
E
Arterial Oxygen Saturation Nadir (%)
F
Minutes to reach 90% BL Arterial Oxygen Saturation
G
Heart Rate Nadir (beats per minute)
H
Minutes to reach 90% BL Heart Rate
I
Respiratory Rate Nadir (breaths per minute)
J
Minutes to reach 90% BL Respiratory Rate
Saline (1ml/kg)
NLXM (1mg/kg)
NLX (1mg/kg)
K Fentanyl (20 µg/kg) + Saline (1ml/kg)
Fentanyl (20 µg/kg) + NLXM (1 mg/kg)
Fentanyl (20 µg/kg) + NLX (1mg/kg)
ts
DMX
L
#Fos-IR nTS neurons
M
%TH-IR nTS cells expressing Fos-IR

918

919 **Figure 4. NLXM-mediated reversal of 20 µg/kg fentanyl-induced respiratory depression is**
920 **comparable to NLX. A.** Schematic showing the timeline for OIRD reversal experiments. Male
921 and Female SD rats underwent jugular catheterization surgery. The following week, conscious
922 rats in their home cages received intravenous fentanyl (20 µg/kg). Four minutes later, rats
923 received intravenous administration (reversal) of either saline (1 ml/kg; n=9), NLX (1 mg/kg;
924 n=9) or NLXM (1 mg/kg; n=12). Cardiorespiratory parameters were measured up to 60 minutes
925 after fentanyl. At the conclusion of the experiment, brains were collected from a subset of
926 animals in each group and processed for Fos- and TH- immunoreactivity. Time course data
927 showing oxygen saturation (**B**), heart rate (**C**) and respiratory rate (**D**) data measurements
928 collected in all groups before and after fentanyl and saline/antagonist administration. Changes
929 in oxygen saturation were assessed as nadir (lowest value; **E,G,I**) and time to recover to 90% of
930 baseline (pre-saline/MOR antagonist; **F,H,J**). In all graphs, males are represented by filled
931 symbols, and females by open symbols. Mean nadir values were assessed in saline-, NLX-, and
932 NLXM-pretreated rats (Oxygen Saturation: One-way ANOVA, $F_{(2,27)} = 0.2916$, $p=0.7494$; Heart
933 Rate: One-way ANOVA, $F_{(2,27)} = 0.4216$, $p=0.6602$; Respiratory Rate: One-way ANOVA, $F_{(2,27)} =$
934 4.679, $p=0.018$; Tukey's post-hoc test, $^{*}p<0.05$. Mean time to reach 90% baseline was
935 assessed for all parameters: Oxygen Saturation: One-way ANOVA, $F_{(2,27)} = 22.58$, $p<0.0001$;
936 Tukey's post-hoc test, $^{****}p<0.0001$; Heart Rate: One-way ANOVA, $F_{(2,27)} = 19.39$, $p<0.0001$;
937 Tukey's post-hoc test, $^{****}p<0.0001$, $^{***}p<0.001$; Respiratory Rate: One-way ANOVA, $F_{(2,27)} =$
938 6.322, $p=0.0001$;Tukey's post-hoc test, $^{**}p<0.01$, $^{*}p<0.05$). **K.** Merged photomicrographs of
939 coronal brainstem sections displaying representative Fos- and TH- immunoreactivity in the nTS
940 of rats that received fentanyl followed by saline, NLX or NLXM. Scale bar = 200 µm. **L.** Mean
941 data of the number of Fos-IR cells evaluated in 3 nTS sections per rat. Number of Fos-IR cells:
942 One-way ANOVA, $F_{(2,15)} = 0.07269$, $p=0.9302$. **M.** Mean data of the percentage of TH-IR cells
943 expressing Fos-IR: One-way ANOVA, $F_{(2,15)} = 3.736$, $p=0.0482$. There were no significant
944 differences in the number of Fos-IR cells or the percentage of TH-IR cells expressing Fos-IR
945 between groups.
946

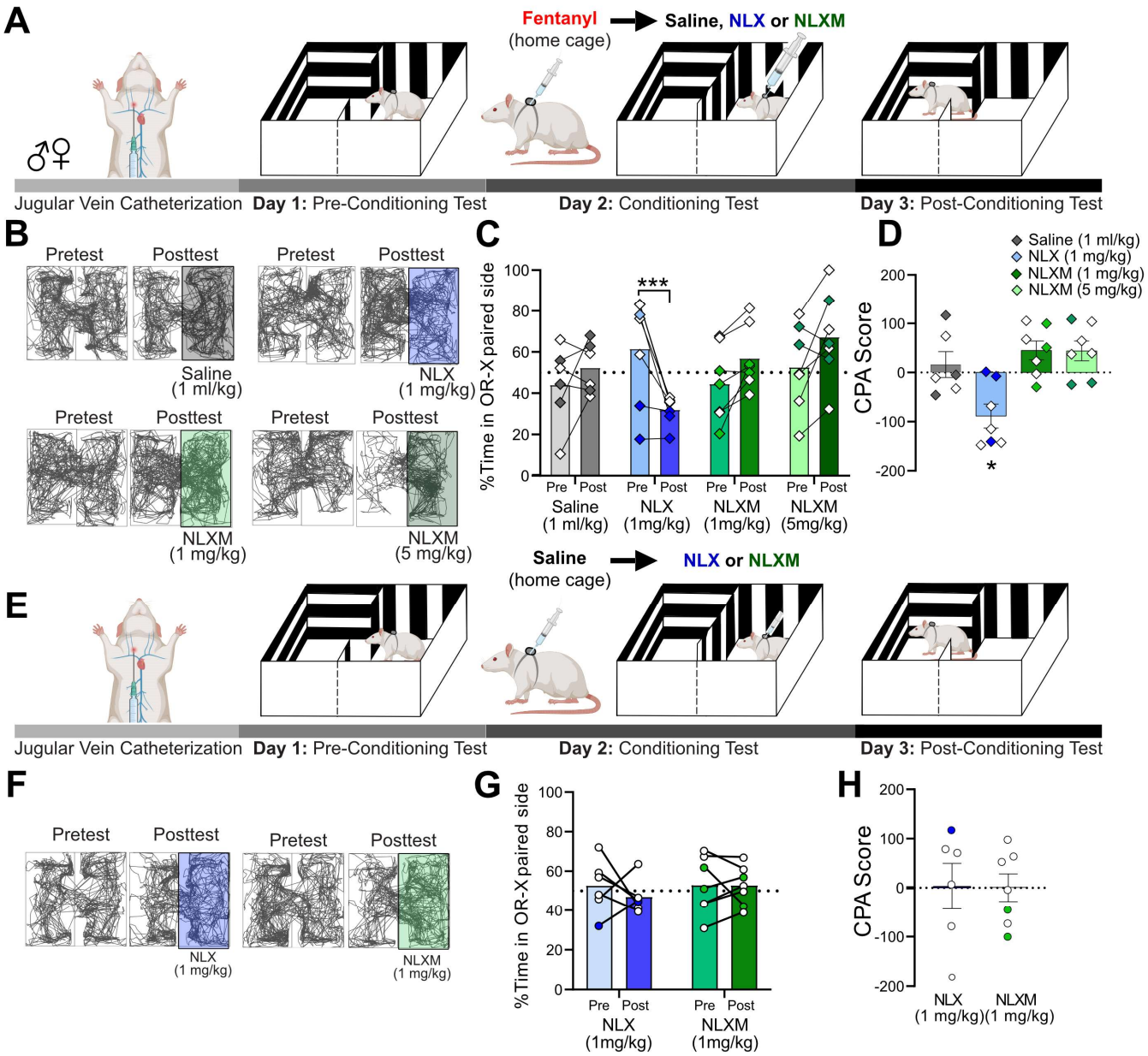
A
Fentanyl
(home cage)
Saline, NLX or NLXM
Jugular Vein Catheterization
Day 1: Pre-Conditioning Test
Day 2: Conditioning Test
Day 3: Post-Conditioning Test
B
Pretest
Posttest
Saline
(1 ml/kg)
NLX
(1 mg/kg)
NLXM
(1 mg/kg)
NLXM
(5 mg/kg)
C
%Time in OR-X paired side
***
Pre
Post
Saline
(1 ml/kg)
NLX
(1mg/kg)
NLXM
(1mg/kg)
NLXM
(5mg/kg)
D
Saline (1 ml/kg)
NLX (1 mg/kg)
NLXM (1 mg/kg)
NLXM (5 mg/kg)
CPA Score
*
Saline
(home cage)
NLX or NLXM
E
Jugular Vein Catheterization
Day 1: Pre-Conditioning Test
Day 2: Conditioning Test
Day 3: Post-Conditioning Test
F
Pretest
Posttest
NLX
(1 mg/kg)
NLXM
(1 mg/kg)
G
%Time in OR-X paired side
Pre
Post
NLX
(1mg/kg)
NLXM
(1mg/kg)
H
CPA Score
NLX
(1 mg/kg)
NLXM
(1 mg/kg)

955 **Figure 5: NLXM-mediated reversal of OIRD is not aversive. A**. Schematic of the Conditioned
956 Place Aversion (CPA) experimental design for rats that received fentanyl followed by saline or
957 an opioid receptor antagonist. Catheterized rats underwent a pre-conditioning test (Day 1). On
958 the conditioning day (Day 2), a divider was placed in the middle of the CPA box. Rats received
959 intravenous fentanyl (50 µg/kg) in their home cages. Four minutes later, rats were transferred to
960 one side of the CPA box and immediately received intravenous saline (1 ml/kg, n=6), NLX (1
961 mg/kg, n=7), or NLXM (1 mg/kg, n=7; 5 mg/kg, n=7). During the post-conditioning test (Day 3),
962 the divider was removed, and rats were placed in the box and allowed to explore both
963 compartments. **B.** Track plot data showing movement in both sides of the CPA box during the
964 Pretest (day 1) and Posttest (Day 3). For each condition, the Pre- and Posttest data is from the
965 same animal. In these representative examples, the saline- or antagonist-paired side is shown
966 on the right side of the box. However, the paired side was balanced between left and right sides
967 of the box for all groups. **C.** Mean data with individual plots showing changes in the time spent
968 in the saline- and antagonist-paired side. In all graphs, males are represented by filled symbols,
969 and females by open symbols. There was a significant decrease in the time spent in the NLX-
970 paired side: two-way repeated measures ANOVA; drug x test interaction: $F_{(3,23)} = 9.994$,
971 p=0.0002; Sidak's post-hoc, ***p=0.0007. **D.** The CPA score (calculated as time spent in the
972 saline or antagonist paired compartment during posttest minus the time spent in the same
973 compartment during the pretest. For CPA scores, one-sample t-test from hypothetical value (no
974 aversion). There was a significant decrease in the CPA score for 1 mg/kg NLX treated rats
975 (t=3.642 (df=6, *p<0.05). 1 mg/kg NLXM: t=2.340, df=6 p=0.0578; 5 mg/kg NLXM: t=2.172,
976 df=6, p=0.0729. Saline, t=0.6113 (df=5, p=0.5677). **E**. Schematic of the Conditioned Place
977 Aversion (CPA) experimental design for saline-pretreated animals. Catheterized rats underwent
978 a pre-conditioning test (Day 1). On the conditioning day (Day 2), a divider was placed in the
979 middle of the CPA box. Rats received intravenous saline (1 ml/kg) in their home cages. Four
980 minutes later, rats were transferred to one side of the CPA box and immediately received
981 intravenous NLX (1 mg/kg, n=6) or NLXM (1 mg/kg, n=7). **F.** Track plot data showing movement
982 in both sides of the CPA box during the Pretest (day 1) and Posttest (Day 3). The paired side
983 was balanced between left and right sides of the box for all groups. **G.** Mean data with individual
984 plots showing changes in the time spent on the NLX- or NLXM-paired side. There was no
985 difference in time spent in the side paired with NLX or NLXM (two-way repeated measures
986 ANOVA, antagonist x time, $F_{(1,11)} = 0.4638$, p=5.099. **H.** CPA scores for NLX- and NLXM-treated
987 animals. There was no significant difference in the CPA scores in rats that received NLX (one

sample t-test, t=0.07102, df=5, p=0.9461) or NLXM (one sample t-test, t=0.005032, df=6, p=0.9961).

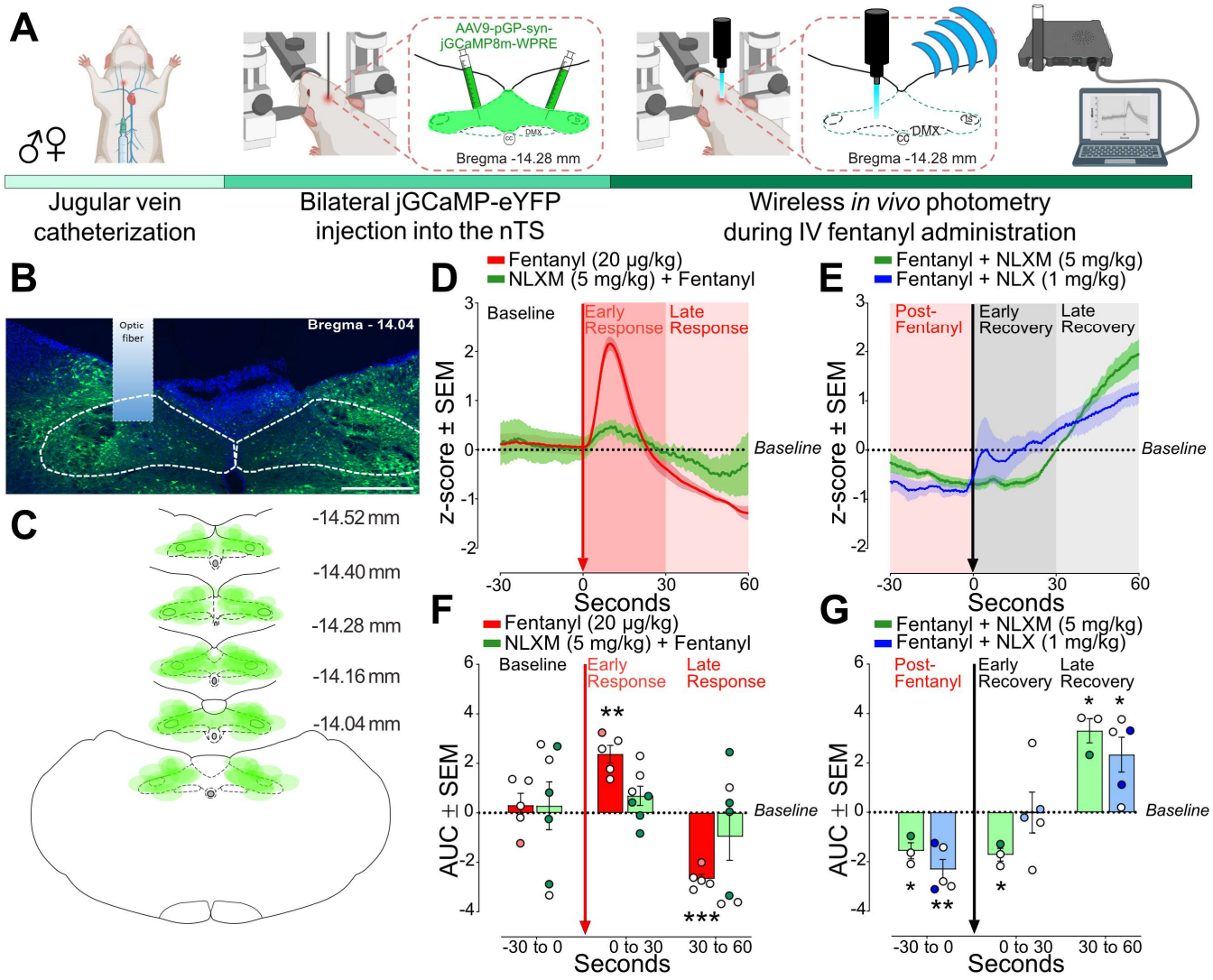
A
AAV9-pGP-syn-jGCaMP8m-WPRE
Bregma -14.28 mm
Bregma -14.28 mm
Jugular vein catheterization
Bilateral jGCaMP-eYFP injection into the nTS
Wireless in vivo photometry during IV fentanyl administration
B
Optic fiber
Bregma - 14.04
C
-14.52 mm
-14.40 mm
-14.28 mm
-14.16 mm
-14.04 mm
D
Fentanyl (20 µg/kg)
NLXM (5 mg/kg) + Fentanyl
Baseline
Early Response
Late Response
z-score ± SEM
Seconds
E
Fentanyl + NLXM (5 mg/kg)
Fentanyl + NLX (1 mg/kg)
Post-Fentanyl
Early Recovery
Late Recovery
F
AUC ± SEM
-30 to 0
0 to 30
30 to 60
G

1007 **Figure 6: Fentanyl-induced nTS activity is mediated by peripheral MORs**.
1008 **A.** Experimental timeline. Male and female rats underwent jugular catheterization surgery,
1009 followed by bilateral nanoinjection of jGCaMP8m into the nTS and then allowed 3-5 weeks for
1010 viral expression. On the test day, rats were anesthetized and placed in a stereotaxic apparatus.
1011 The nTS was exposed and a fiber was lowered into the nTS. **B.** Representative example of
1012 GCaMP expression and fiber placement in the nTS. Scale bar = 200 µm. **C.** Spread of overlay
1013 of individual animal viral expression across the caudal-rostral extent of the nTS. **D.** nTS cell
1014 response (mean z-score) aligned to 20 µg/kg fentanyl administration (red arrow) at Baseline (-
1015 30-0 seconds), early response (0-30 seconds) and late response (30-60 seconds) in rats that
1016 received 20 µg/kg fentanyl only (red trace) or 5 mg/kg NLXM followed by 20 µg/kg fentanyl
1017 (green trace). In all graphs, males are represented by filled symbols, and females by open
1018 symbols. **E.** Area under the curve (AUC) was calculated during baseline (-30 to 0 seconds),
1019 Early Response (0 to 30 seconds) or Late Response (30 to 60 seconds). For AUC graphs, one-
1020 sample t-test from hypothetical zero value. In rats that received fentanyl only, there was a
1021 significant increase in the AUC during the Early Phase (t=6.747, df=4, **p=0.0025) followed by a
1022 significant decrease in the Late Phase (t=14.35, df=4, ***p=0.0001). In rats that received 5
1023 mg/kg NLXM prior to 20 µg/kg fentanyl, no differences in AUC were observed at any time point
1024 (Baseline; t=0.2916, df=6 p=0.7804; Early Phase; t=1.760, df=6 p=0.1288; 30-60 seconds;
1025 t=1.002, df=6, p=0.3548). **F.** nTS cell response (mean z-score) aligned to MOR antagonists
1026 (black arrow). Rats received iv 20 µg/kg fentanyl (Post-Fentanyl phase, -30 to 0 seconds) prior
1027 to MOR antagonist infusion of NLX (1 mg/kg, blue trace) or NLXM (5 mg/kg, green trace). Data
1028 during Early Recovery (0 to 30 seconds) and Late Recovery (30 to 60 seconds) are shown. **G.**
1029 Mean data showing AUC analyses for both groups. For all graphs, one-sample t-test from
1030 hypothetical zero value. NLXM-treated rats had a significant decrease in activity from Post-
1031 Fentanyl baseline prior to NLXM (t=4.799, df=2 * p=0.0408) and during the Early Recovery
1032 phase (t=6.683, df=2 p=0.0217), and exhibited enhanced activity above baseline during the Late
1033 Recovery phase (t=6.716, df=2, * p=0.0215). NLX-treated rats displayed a similar decrease
1034 below baseline prior to NLX. No difference from baseline was observed during the Early
1035 Recovery phase (t=0.01238, df=4 p=0.9907), and a significant increase above baseline was
1036 observed during the Late Recovery phase (t=3.318, df=4, * p=0.0294).
1037
1038
1039
1040